GRID DIAGRAMS AND HEEGAARD FLOER INVARIANTS

CIPRIAN MANOLESCU, PETER S. OZSVÁTH, AND DYLAN P. THURSTON

Abstract. We give combinatorial descriptions of the Heegaard Floer homology groups for arbitrary three-manifolds (with coefficients in $\mathbb{Z}/2\mathbb{Z}$). The descriptions are based on presenting the three-manifold as an integer surgery on a link in the three-sphere, and then using a grid diagram for the link. We also give combinatorial descriptions of the mod 2 Ozsváth-Szabó mixed invariants of closed four-manifolds, also in terms of grid diagrams.

1. Introduction

Starting with the seminal work of Donaldson [3], gauge theory has found numerous applications in low-dimensional topology. Its role is most important in dimension four, where the Donaldson invariants [4], and later the Seiberg-Witten invariants [29, 30, 31], were used to distinguish between homeomorphic four-manifolds that are not diffeomorphic. More recently, Ozsváth and Szabó introduced Heegaard Floer theory [22, 21], an invariant for low-dimensional manifolds inspired by gauge theory, but defined using methods from symplectic geometry. Heegaard Floer invariants in dimension three are known to detect Thurston norm [19] and fiberedness [15]. Heegaard Floer homology can be used to construct various four-dimensional invariants as well [24]. Notable are the so-called mixed invariants, which are conjecturally the same as (the mod two reduction of) the Seiberg-Witten invariants and, further, they are known to share many of their properties: in particular, they are able to distinguish homeomorphic four-manifolds with different smooth structures. In a different direction, there also exist Heegaard Floer invariants for null-homologous knots and links in three-manifolds (see [20, 27, 25]); these have applications to knot theory.

One feature shared by the Donaldson, Seiberg-Witten, and Heegaard Floer invariants is that their original definitions are based on counting solutions to some nonlinear partial differential equations. This makes it difficult to exhibit algorithms which, given a combinatorial presentation of the topological object (for example, a triangulation of the manifold, or a diagram of the knot), calculate the respective invariant. The first such general algorithms appeared in 2006, in the setting of Heegaard Floer theory. Sarkar and Wang [28] gave an algorithm for calculating the hat version of Heegaard Floer homology of three-manifolds. The corresponding maps induced by simply connected cobordisms were calculated in [8]. In a different direction, all versions of the Heegaard Floer homology for links in S^3 were found to be algorithmically computable using *grid diagrams*, see [13]. See also [16, 17, 11] for other developments. This progress notwithstanding, a combinatorial description of the smooth, closed four-manifold invariants remained elusive.

Our aim in this paper is to present combinatorial descriptions of all (completed) versions of Heegaard Floer homology for three-manifolds, as well as of the mixed invariants of closed four-manifolds. It should be noted that we only work with invariants defined over the field $\mathbb{F} = \mathbb{Z}/2\mathbb{Z}$. However, we expect a sign refinement of our descriptions to be possible.

Our strategy is to use (toroidal) grid diagrams to represent links, and to represent three- and four-manifolds in terms of surgeries on those links. Grid diagrams were previously used in [13] to

CM was supported by NSF grant number DMS-0852439, a Clay Research Fellowship, and a Royal Society University Research Fellowship.

PSO was supported by NSF grant number DMS-0804121 and a Guggenheim Fellowship.

DPT was supported by a Sloan Research Fellowship.

give a combinatorial description of link Floer homology. From here one automatically obtains a combinatorial description of the Heegaard Floer homology of Dehn surgeries on knots in S^3, since these are known to be determined by the knot Floer complex, cf. [26, 18]. Since every three-manifold can be expressed as surgery on a link in S^3, it is natural to pursue a similar approach for links.

In [12], the Heegaard Floer homology of an integral surgery on a link is described in terms of some data associated to Heegaard diagrams for the link and its sublinks. In particular, we can consider this description in the case where the Heegaard diagrams come from a grid diagram for the link. For technical reasons, we need to consider slightly different grid diagrams than the ones used in [13] and [14]. Whereas the grids in [13] and [14] had one O marking and one X marking in each row and column, here we will use grids with at least one extra free O marking, that is, a marking such that there are no other markings in the same row or column. (An example of a grid diagram with four free markings is shown on the right hand side of Figure 1.)

In the setting of grids with at least one free marking, the problem of computing the Heegaard Floer homology of surgeries boils down to counting isolated pseudo-holomorphic polygons in the symmetric product of the grid torus. Pseudo-holomorphic bigons of index one are easy to count, as they correspond bijectively to empty rectangles on the grid, cf. [13]. In general, one needs to count $(k+2)$-gons of index $1-k$ that relate the Floer complex of the grid to those of its destabilizations at k points, where $k \geq 0$.

Just as in the case of bigons, one can associate to each polygon a certain object on the grid, which we call an *enhanced domain.* Roughly, an enhanced domain consists of an ordinary domain on the grid plus some numerical data at each destabilization point. (See Definition 3.1 below.) Further, when the enhanced domain is associated to a pseudo-holomorphic polygon, it satisfies certain positivity conditions. (See Definition 3.3 below.) Thus, the problem of counting pseudo-holomorphic polygons reduces to finding the positive enhanced domains of the appropriate index, and counting the number of their pseudo-holomorphic representatives.

When $k = 1$, this problem is almost as simple as in the case $k = 0$. Indeed, the only positive enhanced domains for $k = 1$ are the "snail-like" ones used to construct the destabilization map in [14, Section 3.2], see Figure 6 below. It is not hard to check that each such domain has exactly one pseudo-holomorphic representative, modulo 2.

The key fact that underlies the $k = 1$ calculation is that in that case there exist no positive enhanced domains of index $-k$ corresponding to destabilization at k points. Hence, the positive domains of index $1-k$ are what is called *indecomposable*: in particular, their counts of pseudo-holomorphic representatives depend only on the topology of the enhanced domain (i.e., they are independent of its conformal structure). Unfortunately, this fails to be true for $k \geq 2$: there exist positive enhanced domains of index $-k$, so the counts in index $1-k$ depend on the almost complex structure on the symmetric product of the grid.

Nevertheless, we know that different almost complex structures give rise to chain homotopy equivalent Floer complexes for the surgeries on the link, though they may give different counts for particular domains. Let us think of an almost complex structure as a way of assigning a count (zero or one, modulo 2) to each positive enhanced domain on the grid, in a compatible way. Of course, there may exist other such assignments: we refer to an assignment that satisfies certain compatibility conditions as a *formal complex structure*. (See Definition 4.7 below.) Each formal complex structure produces a model for the Floer complex of the link surgery. If two formal complex structures are homotopic (in a suitable sense, see Definition 4.9), the resulting Floer complexes are chain homotopy equivalent. Suppose now we could show that all formal complex structures on a grid are homotopic. Then, we would easily arrive at a combinatorial formulation for the Floer homology of surgeries. Indeed, one could pick an arbitrary formal complex structure on the grid, which is a combinatorial object; and the homology of the resulting complex would be the right answer, whether or not the formal structure came from an actual almost complex structure on the symmetric product.

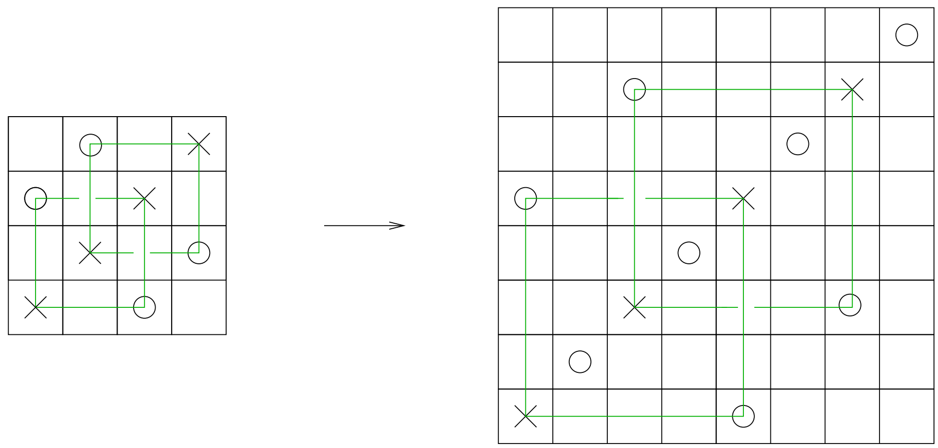

FIGURE 1. **The sparse double.** On the left we show an ordinary grid diagram for the Hopf link, with no free markings. On the right is the corresponding sparse double.

The question of whether or not any two formal complex structures on a grid G are homotopic basically reduces to whether or not a certain cohomology group $HE^d(G)$ vanishes in degrees $d < \min\{0, 2-k\}$. Here, $HE^*(G)$ is the cohomology of a complex generated by positive enhanced domains, modulo periodic domains. (See Definition 4.7.) Computer experimentation suggests the following:

Conjecture 1.1. *Let G be a toroidal grid diagram (with at least one free O marking) representing a link $L \subset S^3$. Then $HE^d(G) = 0$ for any $d < 0$.*

We can prove only a weaker version of this conjecture, but one that is sufficient for our purposes. This version applies only to grid diagrams that are *sparse*, in the sense that if a row contains an X marking, then the adjacent rows do not contain X markings (i.e., they each contain a free O marking); also if a column contains an X marking, then the adjacent columms do not contain X markings. One way to construct a sparse diagram is to start with any grid, and then double its size by interspersing free O markings along a diagonal. The result is called the *sparse double* of the original grid: see Figure 1.

We can show that if G is a sparse grid diagram, then $HE^d(G) = 0$ for $d < \min\{0, 2-k\}$. As a consequence, we obtain:

Theorem 1.2. *Let $\vec{L} \subset S^3$ be an oriented link with a framing Λ. Let $S^3_\Lambda(L)$ be the manifold obtained by surgery on S^3 along (L, Λ), and let $\mathfrak{u}$ be a* Spin^c *structure on $S^3_\Lambda(L)$. Then, given as input a sparse grid diagram for L, the Heegaard Floer homology groups $\mathbf{HF}^-(S^3_\Lambda(L), \mathfrak{u})$, $\mathbf{HF}^\infty(S^3_\Lambda(L), \mathfrak{u})$, $HF^+(S^3_\Lambda(L), \mathfrak{u})$ with coefficients in $\mathbb{F} = \mathbb{Z}/2\mathbb{Z}$ are algorithmically computable.*

The algorithm alluded to in the statement of Theorem 1.2 is given in the proof. In the above statement, $\mathbf{HF}^-$ and $\mathbf{HF}^\infty$ are the completed versions of the usual Heegaard Floer homology groups HF^- and HF^∞, respectively. The groups $\mathbf{HF}^-$ and $\mathbf{HF}^\infty$ are constructed from complexes defined over the power series rings $\mathbb{F}[[U]]$ and $\mathbb{F}[[U, U^{-1}]$, respectively, cf. [12, Section 2], compare also [6]. More precisely, the respective chain complexes are

$$\mathbf{CF}^- = CF^- \otimes_{\mathbb{F}[U]} \mathbb{F}[[U]], \quad \mathbf{CF}^\infty = CF^\infty \otimes_{\mathbb{F}[U,U^{-1}]} \mathbb{F}[[U, U^{-1}].$$

One could also define a completed version of HF^+ in a similar way; but in that case, since multiplication by U is nilpotent on CF^+, the completed version is the same as the original one.

The three completed variants of Heegaard Floer homology are related by a long exact sequence:

$$\cdots \longrightarrow \mathbf{HF}^- \longrightarrow \mathbf{HF}^\infty \longrightarrow HF^+ \longrightarrow \cdots .$$

Moving to four dimensions, in [12] it is shown that every closed four-manifold with $b_2^+ > 1$ admits a description as a three-colored link with a framing. This description is called a link presentation, see Definition 2.8 below.

Theorem 1.3. *Let X be a closed four-manifold with $b_2^+(X) > 1$, and $\mathfrak{s}$ a* Spin^c *structure on X. Given as input a cut link presentation $(\vec{L} = L_1 \cup L_2 \cup L_3, \Lambda)$ for X and a sparse grid diagram for L, one can algorithmically compute the mixed invariant $\Phi_{X,\mathfrak{s}}$ with coefficients in $\mathbb{F} = \mathbb{Z}/2\mathbb{Z}$.*

Although Theorems 1.2 and 1.3 give combinatorial procedures for calculating the respective invariants, in practice our algorithms are very far from being effective. This is especially true since we need to double the size of an ordinary grid in order to arrive at a sparse one. However, one could just assume the truth of Conjecture 1.1, and try to do calculations using any grid with at least one free marking. This is still not effective, and it remains an interesting challenge to modify the algorithm in such a way as to make it more suitable for actual calculations. We remark that, in the case of the hat version of knot Floer homology, the algorithm from [13] has been implemented on computers, see [1, 2, 5]; at present, one can calculate these groups for links with grid number up to 13.

Another application of the methods in this paper is to describe combinatorially the pages of the link surgeries spectral sequence from [23, Theorem 4.1]; see Section 2.12 and Theorem 4.12 below for the relevant discussion. Recall that this spectral sequence can be used to give a relationship between Khovanov homology to the Heegaard Floer homology of branched double covers. In the setting of $\widehat{HF}$, the spectral sequence can also be described combinatorially using bordered Floer homology; see [9], [10].

This paper is organized as follows. In Section 2 we state the results from [12] about how $\mathbf{HF}^-$ of an integral surgery on a link L (and all the related invariants) can be expressed in terms of counts of holomorphic polygon counts on the symmetric product of a grid (with at least one free marking). In Section 3 we define enhanced domains, and associate one to each homotopy class of polygons on the symmetric product. We also introduce the positivity condition on enhanced domains, which is necessary in order for the domain to have holomorphic representatives. In Section 4 we associate to a grid G the complex $CE^*(G)$ whose generators are positive enhanced domains modulo periodic domains. We show that, if Conjecture 1.1 is true, then all possible ways of assigning holomorphic polygon counts to enhanced domains are homotopic. We explain how this would lead to a combinatorial description of the Heegaard Floer invariants. In Section 5 we prove the weaker (but sufficient for our purposes) version of the conjecture, which is applicable to sparse grid diagrams.

Throughout the paper we work over the field $\mathbb{F} = \mathbb{Z}/2\mathbb{Z}$.

Acknowledgement. The first author would like to thank the mathematics department at the University of Cambridge for its hospitality during his stay there in the Spring of 2009. We would also like to thank Robert Lipshitz and Zoltán Szabó for interesting conversations.

2. The surgery theorem applied to grid diagrams

Our main goal here is to present the statement of Theorem 2.5 below, which expresses the Heegaard Floer homology $\mathbf{HF}^-$ of an integral surgery on a link in terms of a grid diagram for the link (or, more precisely, in terms of holomorphic polygon counts on a symmetric product of the grid). We also state similar results for the cobordism maps on $\mathbf{HF}^-$ induced by two-handle additions (Theorem 2.6), for the other completed versions of Heegaard Floer homology (Theorem 2.7), and for the mixed invariants of four-manifolds (Proposition 2.10).

The proofs of all the results from this section are given in [12].

2.1. **Hyperboxes of chain complexes.** We start by summarizing some homological algebra from [12, Section 3].

When f is a function, we denote its n^{th} iterate by $f^{\circ n}$, i.e., $f^{\circ 0} = id,\ f^{\circ 1} = f,\ f^{\circ(n+1)} = f^{\circ n} \circ f$.

For $\mathbf{d} = (d_1, \dots, d_n) \in (\mathbb{Z}_{\geq 0})^n$ a collection of nonnegative integers, we set

$$\mathbb{E}(\mathbf{d}) = \{\varepsilon = (\varepsilon_1, \dots, \varepsilon_n) \mid \varepsilon_i \in \{0, 1, \dots, d_i\},\ i = 1, \dots, n\}.$$

In particular, $\mathbb{E}_n = \mathbb{E}(1, \dots, 1) = \{0, 1\}^n$ is the set of vertices of the n-dimensional unit hypercube.

For $\varepsilon = (\varepsilon_1, \dots, \varepsilon_n) \in \mathbb{E}(\mathbf{d})$, set

$$\|\varepsilon\| = \varepsilon_1 + \cdots + \varepsilon_n.$$

We can view the elements of $\mathbb{E}(\mathbf{d})$ as vectors in $\mathbb{R}^n$. There is a partial ordering on $\mathbb{E}(\mathbf{d})$, given by $\varepsilon' \leq \varepsilon \iff \forall i,\ \varepsilon'_i \leq \varepsilon_i$. We write $\varepsilon' < \varepsilon$ if $\varepsilon' \leq \varepsilon$ and $\varepsilon' \neq \varepsilon$. We say that two multi-indices $\varepsilon, \varepsilon'$ with $\varepsilon \leq \varepsilon'$ are *neighbors* if $\varepsilon' - \varepsilon \in \mathbb{E}_n$, i.e., none of their coordinates differ by more than one.

We define an *n-dimensional hyperbox of chain complexes* $\mathcal{H} = \big((C^\varepsilon)_{\varepsilon \in \mathbb{E}(\mathbf{d})}, (D^\varepsilon)_{\varepsilon \in \mathbb{E}_n}\big)$ of size $\mathbf{d} \in (\mathbb{Z}_{\geq 0})^n$ to consist of a collection of $\mathbb{Z}$-graded vector spaces

$$(C^\varepsilon)_{\varepsilon \in \mathbb{E}(\mathbf{d})}, \quad C^\varepsilon = \bigoplus_{* \in \mathbb{Z}} C^\varepsilon_*,$$

together with a collection of linear maps

$$D^\varepsilon : C^{\varepsilon^0}_* \to C^{\varepsilon^0 + \varepsilon}_{* + \|\varepsilon\| - 1},$$

defined for all $\varepsilon^0 \in \mathbb{E}(\mathbf{d})$ and $\varepsilon \in \mathbb{E}_n$ such that $\varepsilon^0 + \varepsilon \in \mathbb{E}(\mathbf{d})$ (i.e., the multi-indices of the domain and the target are neighbors). The maps D^ε are required to satisfy the relations

$$\sum_{\varepsilon' \leq \varepsilon} D^{\varepsilon - \varepsilon'} \circ D^{\varepsilon'} = 0, \tag{1}$$

for all $\varepsilon \in \mathbb{E}_n$. If $\mathbf{d} = (1, \dots, 1)$, we say that $\mathcal{H}$ is a *hypercube of chain complexes.*

Note that D^ε in principle also depends on ε^0, but we omit that from notation for simplicity. Further, if we consider the total complex

$$C_* = \bigoplus_{\varepsilon \in \mathbb{E}(\mathbf{d})} C^\varepsilon_{* + \|\varepsilon\|},$$

we can think of D^ε as a map from C_* to itself, by extending it to be zero when is not defined. Observe that $D = \sum D^\varepsilon : C_* \to C_{*-1}$ is a chain map.

Let $\mathcal{H} = \big((C^\varepsilon)_{\varepsilon \in \mathbb{E}(\mathbf{d})}, (D^\varepsilon)_{\varepsilon \in \mathbb{E}_n}\big)$ be an n-dimensional hyperbox of chain complexes. Let us imagine the hyperbox $[0, d_1] \times \cdots \times [0, d_n]$ to be split into $d_1 d_2 \cdots d_n$ unit hypercubes. At each vertex ε we see a chain complex $(C^\varepsilon, D^{(0,\dots,0)})$. Associated to each edge of one of the unit hypercubes is a chain map. Along the two-dimensional faces we have chain homotopies between the two possible ways of composing the edge maps, and along higher-dimensional faces we have higher homotopies.

There is a natural way of turning the hyperbox $\mathcal{H}$ into an n-dimensional hypercube $\hat{\mathcal{H}} = (\hat{C}^\varepsilon, \hat{D}^\varepsilon)_{\varepsilon \in \mathbb{E}_n}$, which we called the *compressed hypercube* of $\mathcal{H}$. The compressed hypercube has the property that along its i^{th} edge we see the composition of all the d_i edge maps on the i^{th} axis of the hyperbox.

In particular, if $n = 1$, then $\mathcal{H}$ is a string of chain complexes and chain maps:

$$C^{(0)} \xrightarrow{D^{(1)}} C^{(1)} \xrightarrow{D^{(1)}} \cdots \xrightarrow{D^{(1)}} C^{(d)},$$

and the compressed hypercube $\hat{\mathcal{H}}$ is

$$C^{(0)} \xrightarrow{\left(D^{(1)}\right)^{\circ d}} C^{(d)}.$$

For general n and $\mathbf{d} = (d_1, \dots, d_n)$, the compressed hypercube $\hat{\mathcal{H}}$ has at its vertices the same complexes as those at the vertices of the original hyperbox $\mathcal{H}$:

$$\hat{C}^{(\varepsilon_1,\dots,\varepsilon_n)} = C^{(\varepsilon_1 d_1,\dots,\varepsilon_n d_n)}, \ \varepsilon = (\varepsilon_1, \dots, \varepsilon_n) \in \mathbb{E}_n.$$

If along the i^{th} coordinate axis in $\mathcal{H}$ we have the edge maps $f_i = D^{(0,\dots,0,1,0,\dots,0)}$, then along the respective axis in $\hat{\mathcal{H}}$ we see $f_i^{\circ d_i}$. Given a two-dimensional face of $\mathcal{H}$ with edge maps f_i and f_j and chain homotopies $f_{\{i,j\}}$ between $f_i \circ f_j$ and $f_j \circ f_i$, to the respective compressed face in $\hat{\mathcal{H}}$ we assign the map

$$\sum_{k_i=1}^{d_i} \sum_{k_j=1}^{d_j} f_i^{\circ(k_i-1)} \circ f_j^{\circ(k_j-1)} \circ f_{\{i,j\}} \circ f_j^{\circ(d_j-k_j)} \circ f_i^{\circ(d_i-k_i)},$$

which is a chain homotopy between $f_i^{\circ d_i} \circ f_j^{\circ d_j}$ and $f_j^{\circ d_j} \circ f_i^{\circ d_i}$. The formulas for what we assign to the higher-dimensional faces in $\hat{\mathcal{H}}$ are more complicated, but they always involve sums of compositions of maps in $\mathcal{H}$.

Let ${}^0\mathcal{H}$ and ${}^1\mathcal{H}$ be two hyperboxes of chain complexes, of the same size $\mathbf{d} \in (\mathbb{Z}_{\geq 0})^n$. A *chain map* $F : {}^0\mathcal{H} \to {}^1\mathcal{H}$ is defined to be a collection of linear maps

$$F^{\varepsilon}_{\varepsilon^0} : {}^0C^{\varepsilon^0}_* \to {}^1C^{\varepsilon^0+\varepsilon}_{*+\|\varepsilon\|},$$

satisfying

$$\sum_{\varepsilon' \leq \varepsilon} \bigl(D^{\varepsilon-\varepsilon'}_{\varepsilon^0+\varepsilon'} \circ F^{\varepsilon'}_{\varepsilon^0} + F^{\varepsilon-\varepsilon'}_{\varepsilon^0+\varepsilon'} \circ D^{\varepsilon'}_{\varepsilon^0} \bigr) = 0,$$

for all $\varepsilon^0 \in \mathbb{E}(\mathbf{d}), \varepsilon \in \mathbb{E}_n$ such that $\varepsilon^0 + \varepsilon \in \mathbb{E}(\mathbf{d})$. In particular, F gives an ordinary chain map between the total complexes ${}^0C$ and ${}^1C$.

Starting with from here, we can define chain homotopies and chain homotopy equivalences between hyperboxes by analogy with the usual notions between chain complexes.

The construction of $\hat{\mathcal{H}}$ from $\mathcal{H}$ is natural in the following sense. Given a chain map $F : {}^0\mathcal{H} \to {}^1\mathcal{H}$, there is an induced chain map $\hat{F} : {}^0\hat{\mathcal{H}} \to {}^1\hat{\mathcal{H}}$ between the respective compressed hypercubes. Moreover, if F is a chain homotopy equivalence, then so is $\hat{F}$.

2.2. **Chain complexes from grid diagrams.** Consider an oriented, ℓ-component link $\vec{L} \subset S^3$. We denote the components of $\vec{L}$ by $\{L_i\}_{i=1}^{\ell}$. Let

$$\mathbb{H}(L)_i = \frac{\mathrm{lk}(L_i, L - L_i)}{2} + \mathbb{Z} \subset \mathbb{Q}, \ \ \mathbb{H}(L) = \bigoplus_{i=1}^{\ell} \mathbb{H}(L)_i,$$

where lk denotes linking number. Further, let

$$\overline{\mathbb{H}}(L)_i = \mathbb{H}(L)_i \cup \{-\infty, +\infty\}, \ \ \overline{\mathbb{H}}(L) = \bigoplus_{i=1}^{\ell} \overline{\mathbb{H}}(L)_i.$$

Let G be a toroidal grid diagram representing the link $\vec{L}$ and having at least one free marking, as in [12, Section 12.1]. Precisely, G consists of a torus $\mathcal{T}$, viewed as a square in the plane with the opposite sides identified, and split into n annuli (called rows) by n horizontal circles $\alpha_1, \dots, \alpha_n$, and into n other annuli (called columns) by n vertical circles $\beta_1, \dots, \beta_n$. Further, we are given some markings on the torus, of two types: X and O, such that:

- each row and each column contains exactly one O marking;
- each row and each column contains at most one X marking;
- if the row of an O marking contains no X markings, then the column of that O marking contains no X markings either. An O marking of this kind is called a *free marking.* We assume that the number q of free markings is at least 1.

Observe that G contains exactly n O markings and exactly $n-q$ X markings. A marking that is not free is called *linked*. The number n is called the *grid number* or the *size* of G.

We draw horizontal arcs between the linked markings in the same row (oriented to go from the O to the X), and vertical arcs between the linked markings in the same column (oriented to go from the X to the O). Letting the vertical arcs be overpasses whenever they intersect the horizontal arcs, we obtain a planar diagram for a link in S^3, which we ask to be the given link $\vec{L}$.

We let $\mathbf{S} = \mathbf{S}(G)$ be the set of matchings between the horizontal and vertical circles in G. Any $\mathbf{x} \in \mathbf{S}$ admits a Maslov grading $M(\mathbf{x}) \in \mathbb{Z}$ and an Alexander multi-grading

$$A_i(\mathbf{x}) \in \mathbb{H}(L)_i, \ i \in \{1, \dots, \ell\}.$$

(For the precise formulas for M and A_i, see [14], where they were written in the context of grid diagrams without free markings. However, the same formulas also apply to the present setting.)

For $\mathbf{x}, \mathbf{y} \in \mathbf{S}$, we let $\mathrm{Rect}^\circ(\mathbf{x}, \mathbf{y})$ be the space of empty rectangles between $\mathbf{x}$ and $\mathbf{y}$, as in [14]. Specifically, a *rectangle* from $\mathbf{x}$ to $\mathbf{y}$ is an embedded rectangle r in the torus, whose lower left and upper right corners are coordinates of $\mathbf{x}$, and whose lower right and upper left corners are coordinates of $\mathbf{y}$; and moreover, if all other coordinates of $\mathbf{x}$ coincide with all other coordinates of $\mathbf{y}$. We say that the rectangle is *empty* if its interior contains none of the coordinates of $\mathbf{x}$ (or $\mathbf{y}$).

For $r \in \mathrm{Rect}^\circ(\mathbf{x}, \mathbf{y})$, we denote by $O_j(r)$ and $X_j(r) \in \{0, 1\}$ the number of times O_j (resp. X_j) appears in the interior of r. We can arrange so that the free markings are labeled $O_{n-q+1}, \dots, O_n$. For simplicity, we write

$$F_i(r) = O_{n-q+i}(r), \ i = 1, \dots, q. \tag{2}$$

Let $\mathbb{O}_i$ and $\mathbb{X}_i$ be the set of O's (resp. X's) belonging to the i^{th} component of the link. We fix orderings of the elements of $\mathbb{O}_i$ and $\mathbb{X}_i$, for all i. The i^{th} coordinate of the Alexander multi-grading is characterized uniquely up to an overall additive constant by the property that

$$A_i(\mathbf{x}) - A_i(\mathbf{y}) = \sum_{j \in \mathbb{X}_i} X_j(r) - \sum_{j \in \mathbb{O}_i} O_j(r),$$

where here r is any rectangle from $\mathbf{x}$ to $\mathbf{y}$.

For $i \in \{1, \dots, \ell\}$ and $s \in \overline{\mathbb{H}}(L)_i$, we set

$$E^i_s(r) = \begin{cases} \sum_{j \in \mathbb{O}_i} O_j(r) & \text{if } A_i(\mathbf{x}) \leq s, A_i(\mathbf{y}) \leq s \\ (s - A_i(\mathbf{x})) + \sum_{j \in \mathbb{X}_i} X_j(r) & \text{if } A_i(\mathbf{x}) \leq s, A_i(\mathbf{y}) \geq s \\ \sum_{j \in \mathbb{X}_i} X_j(r) & \text{if } A_i(\mathbf{x}) \geq s, A_i(\mathbf{y}) \geq s \\ (A_i(\mathbf{x}) - s) + \sum_{j \in \mathbb{O}_i} O_j(r) & \text{if } A_i(\mathbf{x}) \geq s, A_i(\mathbf{y}) \leq s. \end{cases}$$

Alternatively, we can write

$$E^i_s(r) = \max(s - A_i(\mathbf{x}), 0) - \max(s - A_i(\mathbf{y}), 0) + \sum_{j \in \mathbb{X}_i} X_j(r) \tag{3}$$

$$= \max(A_i(\mathbf{x}) - s, 0) - \max(A_i(\mathbf{y}) - s, 0) + \sum_{j \in \mathbb{O}_i} O_j(r). \tag{4}$$

In particular, $E^i_{-\infty}(r) = \sum_{j \in \mathbb{X}_i} X_j(r)$ and $E^i_{+\infty}(r) = \sum_{j \in \mathbb{O}_i} O_j(r)$.

Given $\mathbf{s} = (s_1, \dots, s_\ell) \in \overline{\mathbb{H}}(L)$, we define an associated *generalized Floer chain complex* $\mathfrak{A}^-(G, \mathbf{s}) = \mathfrak{A}^-(G, s_1, \dots, s_\ell)$ as follows. $\mathfrak{A}^-(G, \mathbf{s})$ is the free module over $\mathcal{R} = \mathbb{F}[[U_1, \dots, U_{\ell+q}]]$ generated by $\mathbf{S}$, endowed with the differential:

$$\partial \mathbf{x} = \sum_{\mathbf{y} \in \mathbf{S}} \sum_{r \in \mathrm{Rect}^\circ(\mathbf{x}, \mathbf{y})} U_1^{E^1_{s_1}(r)} \cdots U_\ell^{E^\ell_{s_\ell}(r)} \cdot U_{\ell+1}^{F_1(r)} \cdots U_{\ell+q}^{F_q(r)} \mathbf{y}.$$

Note that we can view $\mathfrak{A}^-(G,\mathbf{s})$ as a suitably modified Floer chain complex in $\mathrm{Sym}^n(\mathcal{T})$, equipped with Lagrangian tori $\mathbb{T}_\alpha = \alpha_1 \times \cdots \times \alpha_n$, the product of horizontal circles, and $\mathbb{T}_\beta = \beta_1 \times \cdots \times \beta_n$, the product of vertical circles. The notation $\mathbf{s}$ indicates the way we count powers of U's. Empty rectangles are the same as holomorphic strips of index one in $\mathrm{Sym}^n(\mathcal{T})$, compare [13].

The $\mathfrak{A}^-(G,\mathbf{s})$ can be equipped with a $\mathbb{Z}$-grading $\mu_{\mathbf{s}}$ such that the differential ∂ decreases $\mu_{\mathbf{s}}$ by one. Indeed, when none of the values s_i is $-\infty$, we can set the grading on generators to be

$$\mu_{\mathbf{s}}(\mathbf{x}) = M(\mathbf{x}) - 2\sum_{i=1}^{\ell} \max(A_i(\mathbf{x}) - s_i, 0), \tag{5}$$

and let each U_i decrease grading by 2. When some of the values s_i are $-\infty$, we replace the corresponding expressions $\max(A_i(\mathbf{x}) - s_i, 0)$ by $A_i(\mathbf{x})$ in the Equation (5).

Remark 2.1. When $L = K$ is a knot, the complex $\mathfrak{A}^-(G,s)$ is a multi-basepoint version of the subcomplex $A_s^- = C\{\max(i, j-s) \leq 0\}$ of the knot Floer complex $CFK^\infty(Y,K)$, in the notation of [20]. A similar complex $A_s^+ = C\{\max(i, j-s) \geq 0\}$ appeared in the integer surgery formula in [26], stated there in terms of HF^+ rather than $\mathbf{HF}^-$.

2.3. **Summary of the construction.** For the benefit of the reader, before moving further we include here a short summary of Sections 2.4–2.8 below. The aim of these sections is to be able to state the Surgery Theorem 2.5, which expresses $\mathbf{HF}^-$ of an integral surgery on a link $\vec{L} \subset S^3$ (with framing Λ) as the homology of a certain chain complex $\mathcal{C}^-(G,\Lambda)$ associated to a grid diagram G for $\vec{L}$ (with at least one free marking). Given a sublink $M \subseteq L$, we let G^{L-M} be the grid diagram for $L - M$ obtained from G by deleting all the rows and columns that support components of M. Roughly, the complex $\mathcal{C}^-(G,\Lambda)$ is built as an ℓ-dimensional hypercube of complexes. Each vertex corresponds to a sublink $M \subseteq L$, and the chain complex at that vertex is the direct product of generalized Floer complexes $\mathfrak{A}^-(G^{L-M},\mathbf{s})$, over all possible values $\mathbf{s}$; the reader is encouraged to peek ahead at the expression (18).

The differential on $\mathcal{C}^-(G,\Lambda)$ is a sum of some maps denoted $\Phi^{\vec{M}}_{\mathbf{s}}$, which are associated to oriented sublinks $\vec{M}$: given a sublink M, we need to consider all its possible orientations, not just the one induced from the orientation of $\vec{L}$. When M has only one component, the maps $\Phi^{\vec{M}}_{\mathbf{s}}$ are chain maps going from a generalized Floer complex of $G^{L'}$ (for L' containing M) to one of $G^{L'-M}$. When M has two components, $\Phi^{\vec{M}}_{\mathbf{s}}$ are chain homotopies between different ways of composing the respective chain maps removing one component at a time; for more components of M we get higher homotopies, etc. They fit together in a hypercube of chain complexes, as in Section 2.1.

Each map $\Phi^{\vec{M}}_{\mathbf{s}}$ will be a composition of three kinds of maps, see Equation (14) below: an inclusion map $\mathcal{I}^{\vec{M}}_{\mathbf{s}}$, a "destabilization map" $\hat{D}^{\vec{M}}_{p^{\vec{M}}(\mathbf{s})}$, and an isomorphism $\Psi^{\vec{M}}_{p^{\vec{M}}(\mathbf{s})}$. (Here, $p^{\vec{M}}(\mathbf{s})$ refers to a natural projection from the set $\mathbb{H}(L)$ to itself, see Section 2.5.) The inclusion maps $\mathcal{I}^{\vec{M}}_{\mathbf{s}}$ are defined in Section 2.5, and go between different generalized Floer complexes for the same grid (but different values of $\mathbf{s}$). The destabilization maps $\hat{D}^{\vec{M}}_{\mathbf{s}}$ are defined in Section 2.7, and go from a generalized Floer complex for a grid $G^{L'}$ to one associated to another diagram, which is obtained from the grid by handlesliding some beta curves over others. Finally, the isomorphisms $\Psi^{\vec{M}}_{\mathbf{s}}$ relate these latter complexes to generalized Floer complexes for the smaller grid $G^{L'-M}$; these isomorphisms are defined in Section 2.6.

The main difficulty lies in correctly defining the destabilization maps. When the link M has one component, they are constructed by composing some simpler maps $D^Z_{\mathbf{s}}$. A map $D^Z_{\mathbf{s}}$ corresponds to a single handleslide, done so that the new beta curve encircles a marking $Z \in M$. The type (X or O) of the marking Z is determined by the chosen orientation $\vec{M}$ for M. More generally, we define destabilization maps corresponding to a whole set $\mathcal{Z}$ of markings in Section 2.4 below. When

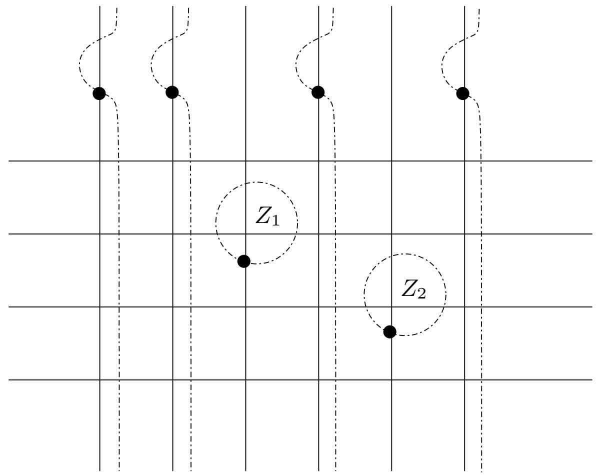

FIGURE 2. **A new collection of curves.** We show here a part of a grid diagram, with the horizontal segments lying on curves in α and the straight vertical segments lying on curves in β. The dashed curves (including the two circles) represent curves in $\beta^{\mathcal{Z}}$, where $\mathcal{Z}$ consists of the two markings Z_1 and Z_2. The maximal degree intersection point $\Theta^{\emptyset,\mathcal{Z}}$ is represented by the black dots.

$\mathcal{Z}$ has two markings, the respective maps $D_{\mathbf{s}}^{\mathcal{Z}}$ are chain homotopies; in general, the maps $D_{\mathbf{s}}^{\mathcal{Z}}$ fit into a hypercube of chain complexes. To construct the destabilization maps for a sublink (which we do in Section 2.7), we build a hyperbox out of maps of the form $D_{\mathbf{s}}^{\mathcal{Z}}$, and apply the compression procedure from Section 2.1.

2.4. **Destabilization at a set of markings.** Let Z be one of the linked markings (of type X or O) on the grid diagram G. We define a subset $J(Z) \subset \overline{\mathbb{H}}(L)$ as follows. If $Z \in \mathbb{O}_i$ for some component L_i, set

$$J(Z) = \{(s_1, \dots, s_\ell) \in \overline{\mathbb{H}}(L) \mid s_i = +\infty\}.$$

If $Z \in \mathbb{X}_i$, set

$$J(Z) = \{(s_1, \dots, s_\ell) \in \overline{\mathbb{H}}(L) \mid s_i = -\infty\}.$$

For $\mathbf{s} \in J(Z)$, note that when we compute powers of U in the chain complex $\mathfrak{A}^-(G, \mathbf{s})$, the other markings in the same column or row as Z do not play any role.

Next, consider a set of linked markings $\mathcal{Z} = \{Z_1, \dots, Z_k\}$. We say that $\mathcal{Z}$ is *consistent* if, for any i, at most one of the sets $\mathcal{Z} \cap \mathbb{O}_i$ and $\mathcal{Z} \cap \mathbb{X}_i$ is nonempty. If $\mathcal{Z}$ is consistent, we set

$$J(\mathcal{Z}) = \bigcap_{i=1}^{k} J(Z_i).$$

If $\mathcal{Z}$ is a consistent set of linked markings, we define a new set of curves $\beta^{\mathcal{Z}} = \{\beta_j^{\mathcal{Z}} \mid j = 1, \dots, n\}$ on the torus $\mathcal{T}$, as follows. Let j_i be the index corresponding to the vertical circle β_{j_i} just to the left of a marking $Z_i \in \mathcal{Z}$. We let $\beta_{j_i}^{\mathcal{Z}}$ be a circle encircling Z_i and intersecting β_{j_i}, as well as the α curve just below Z_i, in two points each; in other words, $\beta_{j_i}^{\mathcal{Z}}$ is obtained from β_j by handlesliding it over the vertical curve just to the right of Z_i. For those j that are not j_i for any $Z_i \in \mathcal{Z}$, we let $\beta_j^{\mathcal{Z}}$ be a curve that is isotopic to β_j, intersects β_j in two points, and does not intersect any of the other beta curves. See Figure 2. (The hypothesis about the existence of at least one free marking is important here, because it ensures that $\beta^{\mathcal{Z}}$ contains at least one vertical beta curve.)

For any consistent collection $\mathcal{Z}$, we denote

$$\mathbb{T}_\beta^{\mathcal{Z}} = \beta_1^{\mathcal{Z}} \times \dots \times \beta_n^{\mathcal{Z}} \subset \mathrm{Sym}^n(\mathcal{T}).$$

The fact that $\mathbf{s} \in J(\mathcal{Z})$ implies that there is a well-defined Floer chain complex $\mathfrak{A}^-(\mathbb{T}_\alpha, \mathbb{T}_\beta^{\mathcal{Z}}, \mathbf{s})$, where the differentials take powers of the U_i's according to $\mathbf{s}$, generalizing the constructions $\mathfrak{A}^-(G, \mathbf{s})$ in a natural manner. More precisely, $\mathfrak{A}^-(\mathbb{T}_\alpha, \mathbb{T}_\beta^{\mathcal{Z}}, \mathbf{s})$ is generated over $\mathcal{R}$ by $\mathbb{T}_\alpha \cap \mathbb{T}_\beta^{\mathcal{Z}}$, with differential given by

$$\partial \mathbf{x} = \sum_{\mathbf{y} \in \mathbb{T}_\alpha \cap \mathbb{T}_\beta^{\mathcal{Z}}} \sum_{\{\phi \in \pi_2(\mathbf{x}, \mathbf{y}) | \mu(\phi) = 1\}} U_1^{E^1_{s_1}(\phi)} \cdots U_\ell^{E^\ell_{s_\ell}(\phi)} \cdot U_{\ell+1}^{F_1(\phi)} \cdots U_{\ell+q}^{F_q(\phi)} \mathbf{y},$$

where $\pi_2(\mathbf{x}, \mathbf{y})$ is the set of homology classes of Whitney disks from $\mathbf{x}$ to $\mathbf{y}$, compare [22], and the functions E^i_s and F_i are as defined in Equations (2), (3) or (4), except we apply them to the domain of ϕ (a two-chain on the torus), rather than to a rectangle.

When we have two collections of linked markings $\mathcal{Z}, \mathcal{Z}'$ such that $\mathcal{Z} \cup \mathcal{Z}'$ is consistent, we require that $\beta_i^{\mathcal{Z}}$ and $\beta_i^{\mathcal{Z}'}$ intersect in exactly two points. As such, there is always a maximal degree intersection point $\Theta^{\mathcal{Z}, \mathcal{Z}'} \in \mathbb{T}_\beta^{\mathcal{Z}} \cap \mathbb{T}_\beta^{\mathcal{Z}'}$.

For each consistent collection of linked markings $\mathcal{Z} = \{Z_1, \dots, Z_m\}$, and each $\mathbf{s} \in J(\mathcal{Z})$, we define an m-dimensional hypercube of chain complexes

$$\mathcal{H}^{\mathcal{Z}}_{\mathbf{s}} = \left(C^{\mathcal{Z}, \varepsilon}_{\mathbf{s}}, D^{\mathcal{Z}, \varepsilon}_{\mathbf{s}} \right)_{\varepsilon \in \mathbb{E}_m}$$

as follows. For $\varepsilon \in \mathbb{E}_m = \{0, 1\}^m$, we let

$$\mathcal{Z}^\varepsilon = \{ Z_i \in \mathcal{Z} \mid \varepsilon_i = 1 \}$$

and set

$$C^{\mathcal{Z}, \varepsilon}_{\mathbf{s}, *} = \mathfrak{A}^-(\mathbb{T}_\alpha, \mathbb{T}_\beta^{\mathcal{Z}^\varepsilon}, \mathbf{s}).$$

For simplicity, we denote $\Theta^{\mathcal{Z}^\varepsilon, \mathcal{Z}^{\varepsilon'}}$ by $\Theta^{\mathcal{Z}}_{\varepsilon, \varepsilon'}$. We write $\varepsilon \prec \varepsilon'$ whenever $\varepsilon, \varepsilon' \in \mathbb{E}_m$ are immediate successors, i.e., $\varepsilon < \varepsilon'$ and $\|\varepsilon' - \varepsilon\| = 1$. For a string of immediate successors $\varepsilon = \varepsilon^0 \prec \varepsilon^1 \prec \cdots \prec \varepsilon^k = \varepsilon'$, we let

$$D^{\mathcal{Z}, \varepsilon^0 \prec \varepsilon^1 \prec \cdots \prec \varepsilon^k}_{\mathbf{s}} : C^{\mathcal{Z}, \varepsilon}_* \to C^{\mathcal{Z}, \varepsilon'}_{*+k-1}, \tag{6}$$

$$D^{\mathcal{Z}, \varepsilon^0 \prec \varepsilon^1 \prec \cdots \prec \varepsilon^k}_{\mathbf{s}}(\mathbf{x}) = \sum_{\mathbf{y} \in \mathbb{T}_\alpha \cap \mathbb{T}_\beta^{\mathcal{Z}^{\varepsilon^k}}} \sum_{\{\phi \in \pi_2(\mathbf{x}, \Theta^{\mathcal{Z}}_{\varepsilon^0, \varepsilon^1}, \dots, \Theta^{\mathcal{Z}}_{\varepsilon^{k-1}, \varepsilon^k}, \mathbf{y}) | \mu(\phi) = 1 - k\}} \big(\# \mathcal{M}(\phi) \big) \cdot U_1^{E^1_{s_1}(\phi)} \cdots U_\ell^{E^\ell_{s_\ell}(\phi)} \cdot U_{\ell+1}^{F_1(r)} \cdots U_{\ell+q}^{F_q(r)} \mathbf{y}$$

be the map defined by counting isolated pseudo-holomorphic polygons in the symmetric product $\mathrm{Sym}^n(\mathcal{T})$. Here,

$$\pi_2(\mathbf{x}, \Theta^{\mathcal{Z}}_{\varepsilon^0, \varepsilon^1}, \dots, \Theta^{\mathcal{Z}}_{\varepsilon^{k-1}, \varepsilon^k}, \mathbf{y})$$

denotes the set of homotopy classes of polygons with edges on $\mathbb{T}_\alpha, \mathbb{T}_\beta^{\mathcal{Z}^{\varepsilon^0}}, \dots, \mathbb{T}_\beta^{\mathcal{Z}^{\varepsilon^k}}$, in this cyclic order, and with the specified vertices. The number $\mu(\phi) \in \mathbb{Z}$ is the Maslov index, and $\mathcal{M}(\phi)$ is the moduli space of holomorphic polygons in the class ϕ. The Maslov index has to be $1 - k$ for the expected dimension of the moduli space of polygons to be zero. This is because the moduli space of conformal structures on a disk with $k + 2$ marked points has dimension $(k + 2) - 3 = k - 1$. Note that this definition of μ is different from the one in [23, Section 4.2], where it denoted expected dimension.

In the special case $k = 0$, we need to divide $\mathcal{M}(\phi)$ by the action of $\mathbb{R}$ by translations; the resulting $D^{\mathcal{Z}, \varepsilon^0}$ is the usual differential ∂.

Define

$$D^{\mathcal{Z}, \varepsilon}_{\mathbf{s}} : C^{\mathcal{Z}, \varepsilon^0}_* \to C^{\mathcal{Z}, \varepsilon^0 + \varepsilon}_{*+k-1}, \quad D^{\mathcal{Z}, \varepsilon}_{\mathbf{s}} = \sum_{\varepsilon^0 \prec \varepsilon^1 \prec \cdots \prec \varepsilon^k = \varepsilon^0 + \varepsilon} D^{\mathcal{Z}, \varepsilon^0 \prec \varepsilon^1 \prec \cdots \prec \varepsilon^k}_{\mathbf{s}}. \tag{7}$$

$$\begin{tikzcd}
 & \mathfrak{A}^-(\mathbb{T}_\alpha, \mathbb{T}_\beta, \mathbf{s}) \arrow[dl, "D_{\mathbf{s}}^{(Z_1)}"'] \arrow[dr, "D_{\mathbf{s}}^{(Z_2)}"] \arrow[dd, bend right, "\begin{array}{l} D_{\mathbf{s}}^{\{Z_1,Z_2\}} = \\ D_{\mathbf{s}}^{(Z_1,Z_2)} + D_{\mathbf{s}}^{(Z_2,Z_1)} \end{array}"] & \\
\mathfrak{A}^-(\mathbb{T}_\alpha, \mathbb{T}_\beta^{(Z_1)}, \mathbf{s}) \arrow[dr, "D_{\mathbf{s}}^{(Z_2)}"'] & & \mathfrak{A}^-(\mathbb{T}_\alpha, \mathbb{T}_\beta^{(Z_2)}, \mathbf{s}) \arrow[dl, "D_{\mathbf{s}}^{(Z_1)}"] \\
 & \mathfrak{A}^-(\mathbb{T}_\alpha, \mathbb{T}_\beta^{(Z_1 Z_2)}, \mathbf{s}) &
\end{tikzcd}$$

FIGURE 3. **Destabilization maps for two linked markings.** The straight lines represent chain maps corresponding to destabilization at one marking, and the curved map is a chain homotopy between the two compositions. Each chain map $D_{\mathbf{s}}^{(Z_i)}$ could also have been written as $D_{\mathbf{s}}^{\{Z_i\}}$.

The following is a particular case of [12, Lemma 6.12]; compare also [22, Lemma 9.7] and [23, Lemma 4.3]:

Lemma 2.2. *For any consistent collection $\mathcal{Z} = \{Z_1, \dots, Z_m\}$ and $\mathbf{s} \in J(\mathcal{Z})$, the resulting $\mathcal{H}_{\mathbf{s}}^{\mathcal{Z}} = (C_{\mathbf{s}}^{\mathcal{Z},\varepsilon}, D_{\mathbf{s}}^{\mathcal{Z},\varepsilon})_{\mathbf{s}\in\mathbb{E}_m}$ is a hypercube of chain complexes.*

Remark 2.3. For future reference, it is helpful to introduce a different notation for the maps (6) and (7). First, let us look at (6) in the case $k = m$, $\varepsilon^0 = (0, \dots, 0)$ and $\varepsilon^m = (1, \dots, 1)$. A string of immediate successors $\varepsilon^0 \prec \dots \prec \varepsilon^m$ is the same as a re-ordering $(Z_{\sigma(1)}, \dots, Z_{\sigma(m)})$ of $\mathcal{Z} = \{Z_1, \dots, Z_m\}$, according to the permutation σ in the symmetric group S_m such that

$$\mathcal{Z}^{\varepsilon^i} = \mathcal{Z}^{\varepsilon^{i-1}} \cup \{Z_{\sigma(i)}\}.$$

We then write:

$$D_{\mathbf{s}}^{(Z_{\sigma(1)},\dots,Z_{\sigma(m)})} = D_{\mathbf{s}}^{\mathcal{Z},\varepsilon^0\prec\varepsilon^1\prec\dots\prec\varepsilon^k}.$$

In particular, we let $D_{\mathbf{s}}^{(\mathcal{Z})} = D_{\mathbf{s}}^{(Z_1,\dots,Z_m)}$ be the map corresponding to the identity permutation. Further, we write $D_{\mathbf{s}}^{\mathcal{Z}}$ for the longest map $D_{\mathbf{s}}^{\mathcal{Z},(1,\dots,1)}$ in the hypercube $\mathcal{H}_{\mathbf{s}}^{\mathcal{Z}}$, that is,

$$D_{\mathbf{s}}^{\mathcal{Z}} = \sum_{\sigma\in S_m} D_{\mathbf{s}}^{(Z_{\sigma(1)},\dots,Z_{\sigma(m)})}. \tag{8}$$

Observe that $D_{\mathbf{s}}^{\mathcal{Z}}$, unlike $D_{\mathbf{s}}^{(\mathcal{Z})}$, is independent of the ordering of $\mathcal{Z}$. Observe also that an arbitrary map $D_{\mathbf{s}}^{\mathcal{Z},\varepsilon}$ from $\mathcal{H}_{\mathbf{s}}^{\mathcal{Z}}$ is the same as the longest map $D_{\mathbf{s}}^{\mathcal{Z}^\varepsilon}$ in a sub-hypercube of $\mathcal{H}_{\mathbf{s}}^{\mathcal{Z}}$. In this notation, the result of Lemma 2.2 can be written as:

$$\sum_{\mathcal{Z}'\subseteq\mathcal{Z}} D_{\mathbf{s}}^{\mathcal{Z}\setminus\mathcal{Z}'} \circ D_{\mathbf{s}}^{\mathcal{Z}} = 0.$$

See Figure 3 for a picture of the hypercube corresponding to destabilization at a set $\mathcal{Z} = \{Z_1, Z_2\}$ of two linked markings.

2.5. **Sublinks and inclusion maps.** Suppose that $M \subseteq L$ is a sublink. We choose an orientation on M (possibly different from the one induced from $\vec{L}$), and denote the corresponding oriented link by $\vec{M}$. We let $I_+(\vec{L}, \vec{M})$ (resp. $I_-(\vec{L}, \vec{M})$) to be the set of indices i such that the component L_i is in M and its orientation induced from $\vec{L}$ is the same as (resp. opposite to) the one induced from $\vec{M}$.

For $i \in \{1, \dots, \ell\}$, we define a map $p_i^{\vec{M}} : \overline{\mathbb{H}}(L)_i \to \overline{\mathbb{H}}(L)_i$ by

$$p_i^{\vec{M}}(s) = \begin{cases} +\infty & \text{if } i \in I_+(\vec{L}, \vec{M}), \\ -\infty & \text{if } i \in I_-(\vec{L}, \vec{M}), \\ s & \text{otherwise.} \end{cases}$$

Then, for $\mathbf{s} = (s_1, \dots, s_\ell) \in \overline{\mathbb{H}}(L)$, we set

$$p^{\vec{M}}(\mathbf{s}) = \big(p_1^{\vec{M}}(s_1), \dots, p_\ell^{\vec{M}}(s_\ell)\big).$$

and define an inclusion map

$$\mathcal{I}_{\mathbf{s}}^{\vec{M}} : \mathfrak{A}^-(G, \mathbf{s}) \to \mathfrak{A}^-(G, p^{\vec{M}}(\mathbf{s}))$$

by

$$\mathcal{I}_{\mathbf{s}}^{\vec{M}} \mathbf{x} = \prod_{i \in I_+(\vec{L}, \vec{M})} U_i^{\max(A_i(\mathbf{x}) - s_i, 0)} \cdot \prod_{i \in I_-(\vec{L}, \vec{M})} U_i^{\max(s_i - A_i(\mathbf{x}), 0)} \cdot \mathbf{x}. \tag{9}$$

provided the exponents are finite, that is, $s_i \neq -\infty$ for all $i \in I_+(\vec{L}, \vec{M})$, and $s_i \neq +\infty$ for all $i \in I_-(\vec{L}, \vec{M})$. These conditions will always be satisfied when we consider inclusion maps in this paper.

Equations (3) and (4) imply that $\mathcal{I}_{\mathbf{s}}^{\vec{M}}$ is a chain map.

Let N be the complement of the sublink M in L. We define a reduction map

$$\psi^{\vec{M}} : \overline{\mathbb{H}}(L) \longrightarrow \overline{\mathbb{H}}(N) \tag{10}$$

as follows. The map $\psi^{\vec{M}}$ depends only on the summands $\overline{\mathbb{H}}(L)_i$ of $\overline{\mathbb{H}}(L)$ corresponding to $L_i \subseteq N$. Each of these L_i's appears in N with a (possibly different) index j_i, so there is a corresponding summand $\overline{\mathbb{H}}(N)_{j_i}$ of $\overline{\mathbb{H}}(N)$. We then set

$$\psi_i^{\vec{M}} : \overline{\mathbb{H}}(L)_i \to \overline{\mathbb{H}}(N)_{j_i}, \quad s_i \mapsto s_i - \frac{\mathrm{lk}(L_i, \vec{M})}{2},$$

where L_i is considered with the orientation induced from L, while $\vec{M}$ is with its own orientation. We then define $\psi^{\vec{M}}$ to be the direct sum of the maps $\psi_i^{\vec{M}}$, pre-composed with projection to the relevant factors. Note that $\psi^{\vec{M}} = \psi^{\vec{M}} \circ p^{\vec{M}}$.

2.6. **Destabilized complexes.** Let $\mathcal{Z} = \{Z_1, \dots, Z_m\}$ be a consistent set of linked markings, and pick $\mathbf{s} \in J(\mathcal{Z})$. In Section 2.4 we introduced a Floer complex $\mathfrak{A}^-(\mathbb{T}_\alpha, \mathbb{T}_\beta^{\mathcal{Z}}, \mathbf{s})$ based on counting holomorphic curves. Our next goal is to describe this complex combinatorially.

Let $L(\mathcal{Z}) \subseteq L$ be the sublink consisting of those components L_i such that at least one of the markings on L_i is in $\mathcal{Z}$. We orient $L(\mathcal{Z})$ as $\vec{L}(\mathcal{Z})$, such that a component L_i is given the orientation coming from $\vec{L}$ when $\mathcal{Z} \cap \mathbb{O}_i \neq \emptyset$, and is given the opposite orientation when $\mathcal{Z} \cap \mathbb{X}_i \neq \emptyset$. Moreover, we let $L((\mathcal{Z})) \subseteq L$ be the sublink consisting of the components L_i such that either all X or all O markings on L_i are in $\mathcal{Z}$.

Consider the grid diagram $G^{\mathcal{Z}}$ obtained from G by deleting the markings in $\mathbb{X}_i$ when $\mathcal{Z} \cap \mathbb{O}_i \neq \emptyset$, deleting the markings in $\mathbb{O}_i$ when $\mathcal{Z} \cap \mathbb{X}_i \neq \emptyset$, and finally deleting the rows and columns containing the markings in $\mathcal{Z}$. The former free O markings in G remain as free markings in $G^{\mathcal{Z}}$. However, in $G^{\mathcal{Z}}$ there may be some additional free markings, coming from linked O or X markings in G that

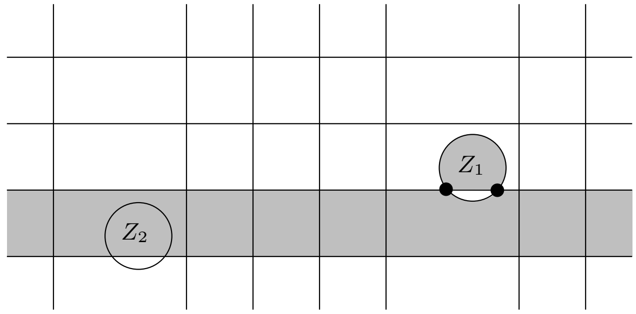

FIGURE 4. **The complex $\mathcal{K}(\mathcal{Z})$.** The figure shows part of a grid diagram with some arcs on the α and $\beta^{\mathcal{Z}}$ curves drawn. There are two intersection points (marked as bullets) between the alpha curve below the marking $Z_1 \in \mathcal{Z}$, and the corresponding beta curve. There are two differentials going from the left to the right generator: a bigon containing Z_1 and an annulus containing Z_2, both drawn shaded in the diagram. This produces one of the factors in the definition of the complex $\mathcal{K}(\mathcal{Z})$.

were not in $\mathcal{Z}$, but were on the same link component as a marking in $\mathcal{Z}$. To be consistent with our previous conventions, we relabel all the newly free X markings as O's.

Thus, $G^{\mathcal{Z}}$ becomes a grid diagram (with free markings) for the link $L-L(\mathcal{Z})$, with the orientation induced from $\vec{L}$. We define complexes $\mathfrak{A}^-(G^{\mathcal{Z}}, \mathbf{s})$ for $\mathbf{s} \in J(\mathcal{Z})$ as in Section 2.2, but rather than assigning a separate U variable to each newly free marking, we keep track of these markings using the same U variables they had in G. This way we lose the variables U_i for $L_i \subseteq L((\mathcal{Z}))$, so the complex $\mathfrak{A}^-(G^{\mathcal{Z}}, \mathbf{s})$ is naturally defined over the free power series ring in the variables U_i for $i = 1, \dots, \ell$ with $L_i \nsubseteq L((\mathcal{Z}))$, as well as $U_{\ell+1}, \dots, U_{\ell+q}$. Note that holomorphic disks of index one in the symmetric product of $G^{\mathcal{Z}}$ are in one-to-one correspondence with rectangles on $G^{\mathcal{Z}}$.

For $Z \in \mathcal{Z}$, let $j(Z) \in \{1, \dots, \ell\}$ be such that $L_{j(Z)}$ is the component of L containing Z, and let $j(Z)'$ correspond to the component $L_{j(Z)'}$ containing the markings in the row exactly under the row through Z. We define a complex

$$\mathcal{K}(\mathcal{Z}) = \bigotimes_{Z \in \mathcal{Z}} \Big(\mathcal{R} \xrightarrow{U_{j(Z)} - U_{j(Z)'}} \mathcal{R} \Big).$$

Using the argument in [12, Proposition 12.2], for a suitable choice of almost complex structure on the symmetric product $\mathrm{Sym}^n(\mathcal{T})$, we have an isomorphism

$$\Psi_{\mathbf{s}}^{\mathcal{Z}} : \mathfrak{A}^-(\mathbb{T}_\alpha, \mathbb{T}_\beta^{\mathcal{Z}}, \mathbf{s}) \to \mathfrak{A}^-(G^{\mathcal{Z}}, \psi^{\vec{L}(\mathcal{Z})}(\mathbf{s}))[[\{U_i\}_{L_i \subseteq L((\mathcal{Z}))}]] \otimes_{\mathcal{R}} \mathcal{K}(\mathcal{Z}). \tag{11}$$

Here, the map $\psi^{\vec{L}(\mathcal{Z})} : \overline{\mathbb{H}}(L) \longrightarrow \overline{\mathbb{H}}(L - L(\mathcal{Z}))$ is as in Equation (10).

To get an understanding of Equation (11), note that there is a clear one-to-one correspondence between the generators of each side. The differentials correspond likewise: on the left hand side, apart from rectangles, we also have for example annuli as the one shown in Figure 4, which give rise to the factors in the complex $\mathcal{K}(\mathcal{Z})$.

For a generic almost complex structure on the symmetric product, we still have a map $\Psi_{\mathbf{s}}^{\mathcal{Z}}$, but this is a chain homotopy equivalence rather than an isomorphism.

A particular instance of the discussion above appears when we have a sublink $M \subseteq L$, with some orientation $\vec{M}$. We then set

$$\mathcal{Z}(\vec{M}) = \bigcup_{i \in I_+(\vec{L}, \vec{M})} \mathbb{O}_i \cup \bigcup_{i \in I_-(\vec{L}, \vec{M})} \mathbb{X}_i.$$

Note that $\vec{L}(\mathcal{Z}(\vec{M})) = \vec{M}$. In this setting, the destabilized grid diagram $G^{L-M} = G^{\mathcal{Z}(\vec{M})}$ is obtained from G by eliminating all rows and columns on which M is supported. It represents the link $L - M$.

For simplicity, we denote

$$\mathcal{K}(\vec{M}) = \mathcal{K}(\mathcal{Z}(\vec{M})), \quad J(\vec{M}) = J(\mathcal{Z}(\vec{M})),$$

and, for $\mathbf{s} \in J(\vec{M})$,

$$\Psi^{\vec{M}}_{\mathbf{s}} = \Psi^{\mathcal{Z}(\vec{M})}_{\mathbf{s}} : \mathfrak{A}^-(\mathbb{T}_\alpha, \mathbb{T}^{\mathcal{Z}(\vec{M})}_\beta, \mathbf{s}) \to \mathfrak{A}^-(G^{L-M}, \psi^{\vec{M}}(\mathbf{s}))[[\{U_i\}_{L_i \subseteq M}]] \otimes_{\mathcal{R}} \mathcal{K}(\vec{M}). \tag{12}$$

2.7. **Destabilization of a sublink.** Let $M \subseteq L$ be a sublink, endowed with an arbitrary orientation $\vec{M}$. For any $\mathbf{s} \in J(\vec{M}) = J(\mathcal{Z}(\vec{M}))$, we construct a hyperbox of chain complexes $\mathcal{H}^{\vec{L},\vec{M}}_{\mathbf{s}}$, as follows. Order the components of M according to their ordering as components of L:

$$M = L_{i_1} \cup \dots \cup L_{i_m}, \quad i_1 < \dots < i_m.$$

For $j = 1, \dots, m$, let us denote $M_j = L_{i_j}$ for simplicity, and equip M_j with the orientation $\vec{M}_j$ induced from $\vec{M}$. Then $\mathcal{Z}(\vec{M}_j)$ is either $\mathbb{O}_{i_j}$ or $\mathbb{X}_{i_j}$. In either case, we have an ordering of its elements, so we can write

$$\mathcal{Z}(\vec{M}_j) = \{Z^{\vec{M}_j}_1, \dots, Z^{\vec{M}_j}_{d_j}\},$$

where d_j is the cardinality of $\mathcal{Z}(\vec{M}_j)$.

The hyperbox $\mathcal{H}^{\vec{L},\vec{M}}_{\mathbf{s}}$ is m-dimensional, of size $\mathbf{d}^M = (d_1, \dots, d_m)$. For each multi-index $\varepsilon = (\varepsilon_1, \dots, \varepsilon_m) \in \mathbb{E}(\mathbf{d}^M)$, we let $\mathcal{Z}(\vec{M})^\varepsilon \subseteq \mathcal{Z}(\vec{M})$ be the collection of markings

$$\mathcal{Z}(\vec{M})^\varepsilon = \bigcup_{j=1}^m \{Z^{\vec{M}_j}_1, \dots, Z^{\vec{M}_j}_{\varepsilon_j}\}.$$

We then let

$$\beta^\varepsilon = \beta^{\mathcal{Z}(\vec{M})^\varepsilon}$$

be the collection of beta curves destabilized at the points of $\mathcal{Z}(\vec{M})^\varepsilon$. For each ε, consider the Heegaard diagram $\mathcal{H}^{\vec{L},\vec{M}}_\varepsilon = (\mathcal{T}, \alpha, \beta^\varepsilon)$, with the z basepoints being the markings in $\mathbb{X}_i$ for $L_i \not\subseteq M$, and the w basepoints being the markings in $\mathcal{Z}(\vec{M})$, together with those in $\mathbb{O}_i$ for $L_i \not\subseteq M$. This diagram represents the link $\vec{L} - M$.

At each vertex $\varepsilon \in \mathbb{E}(\mathbf{d}^M)$ we place the Floer complex

$$C^{\vec{L},\vec{M},\varepsilon}_{\mathbf{s}} = \mathfrak{A}^-(\mathbb{T}_\alpha, \mathbb{T}^{\mathcal{Z}(\vec{M})^\varepsilon}_\beta, \mathbf{s}),$$

and along the faces we have linear maps

$$D^{\vec{L},\vec{M},\varepsilon'}_{\mathbf{s}} = D^{\mathcal{Z}(\vec{M})^\varepsilon,\varepsilon'}_{\mathbf{s}}, \ \varepsilon' \in \mathbb{E}_m \subseteq \mathbb{E}(\mathbf{d}^M),$$

where $D^{\mathcal{Z}(\vec{M})^\varepsilon,\varepsilon'}_{\mathbf{s}}$ are as in (7) above.

We compress the hyperbox of Floer complexes associated to $\mathcal{H}^{\vec{L},\vec{M}}_{\mathbf{s}}$, cf. Section 2.1, and define

$$\hat{D}^{\vec{M}}_{\mathbf{s}} : \mathfrak{A}^-(G, \mathbf{s}) \to \mathfrak{A}^-(\mathbb{T}_\alpha, \mathbb{T}^{\mathcal{Z}(\vec{M})}_\beta, \mathbf{s}). \tag{13}$$

to be the longest diagonal map in the compressed hypercube $\hat{\mathcal{H}}^{\vec{L},\vec{M}}_{\mathbf{s}}$.

For example, when $M = L_i$ is a single component, the map $\hat{D}^{\vec{M}}_{\mathbf{s}}$ is a composition of the triangle maps corresponding to handleslides over the basepoints in $\mathcal{Z}(\vec{M})$, in the given order. When M has several components, it is a composition of more complicated polygon maps, corresponding to chain homotopies (of higher order) between compositions of the handleslide maps.

Note that for each $\mathbf{s} \in \mathbb{H}(L)$, we have $p^{\vec{M}}(\mathbf{s}) \in J(\mathcal{Z}(\vec{M}))$ by definition. Therefore, by composing the maps (9), (13) and (12) (the latter two taken with respect to $p^{\vec{M}}(\mathbf{s})$ rather than $\mathbf{s}$), we obtain a map

$$\begin{aligned} &\Phi^{\vec{M}}_{\mathbf{s}} : \mathfrak{A}^-(G, \mathbf{s}) \longrightarrow \mathfrak{A}^-(G^{L-M}, \psi^{\vec{M}}(\mathbf{s}))[[\{U_i\}_{L_i \subseteq M}]] \otimes_{\mathcal{R}} \mathcal{K}(\vec{M}), \\ &\Phi^{\vec{M}}_{\mathbf{s}} = \Psi^{\vec{M}}_{p^{\vec{M}}(\mathbf{s})} \circ \hat{D}^{\vec{M}}_{p^{\vec{M}}(\mathbf{s})} \circ \mathcal{I}^{\vec{M}}_{\mathbf{s}}, \end{aligned} \tag{14}$$

defined for any $\mathbf{s} \in \overline{\mathbb{H}}(L)$.

For simplicity, let us denote

$$D^{\vec{M}}_{\mathbf{s}} = \Psi^{\vec{M}}_{\mathbf{s}} \circ \hat{D}^{\vec{M}}_{\mathbf{s}} : \mathfrak{A}^-(G, \mathbf{s}) \to \mathfrak{A}^-(G^{L-M}, \psi^{\vec{M}}(\mathbf{s}))[[\{U_i\}_{L_i \subseteq M}]] \otimes_{\mathcal{R}} \mathcal{K}(\vec{M}). \tag{15}$$

The following is a variant of [12, Proposition 7.4], discussed in the proof of [12, Proposition 12.6]:

Lemma 2.4. *Let $M_1, M_2 \subseteq L$ be two disjoint sublinks, with orientations $\vec{M}_1$ and $\vec{M}_2$. For any $\mathbf{s} \in J(\vec{M}_1)$, we have:*

$$\mathcal{I}^{\vec{M}_2}_{\psi^{\vec{M}_1}(\mathbf{s})} \circ D^{\vec{M}_1}_{\mathbf{s}} = D^{\vec{M}_1}_{p^{\vec{M}_2}(\mathbf{s})} \circ \mathcal{I}^{\vec{M}_2}_{\mathbf{s}}. \tag{16}$$

For any $\vec{M}$ and $\mathbf{s} \in \overline{\mathbb{H}}(L)$, by applying Lemma 2.4 and the properties of compression from Section 2.1, we get:

$$\sum_{\vec{M}_1 \amalg \vec{M}_2 = \vec{M}} \Phi^{\vec{M}_2}_{\psi^{\vec{M}_1}(\mathbf{s})} \circ \Phi^{\vec{M}_1}_{\mathbf{s}} = 0, \tag{17}$$

where $\vec{M}_1$ and $\vec{M}_2$ are considered with the orientations induced from $\vec{M}$. See [12, Proposition 12.6].

2.8. **The surgery theorem.** Let us fix a framing Λ for the link $\vec{L}$. For a component L_i of L, we let Λ_i be its induced framing, thought of as an element in $H_1(Y - L)$. This last group can be identified with $\mathbb{Z}^\ell$ using the basis of oriented meridians for the components. Under this identification, for $i \neq j$, the j^{th} component of the vector Λ_i is the linking number between L_i and L_j. The i^{th} component of Λ_i is its homological framing coefficient of L_i as a knot.

Given a sublink $N \subseteq L$, we let $\Omega(N)$ be the set of all possible orientations on N. For $\vec{N} \in \Omega(N)$, we let

$$\Lambda_{\vec{L},\vec{N}} = \sum_{i \in I_-(\vec{L},\vec{N})} \Lambda_i \in \mathbb{Z}^\ell.$$

We consider the $\mathcal{R}$-module

$$\mathcal{C}^-(G, \Lambda) = \bigoplus_{M \subseteq L} \prod_{\mathbf{s} \in \mathbb{H}(L)} \Big(\mathfrak{A}^-(G^{L-M}, \psi^M(\mathbf{s}))[[\{U_i\}_{L_i \subseteq M}]] \Big) \otimes_{\mathcal{R}} \mathcal{K}(M), \tag{18}$$

where ψ^M simply means $\psi^{\vec{M}}$ with $\vec{M}$ being the orientation induced from the one on $\vec{L}$.

We equip $\mathcal{C}^-(G, \Lambda)$ with a boundary operator $\mathcal{D}^-$ as follows.

For $\mathbf{s} \in \mathbb{H}(L)$ and $\mathbf{x} \in \big(\mathfrak{A}^-(G^{L-M}, \psi^M(\mathbf{s}))[[\{U_i\}_{L_i \subseteq M}]]\big) \otimes_{\mathcal{R}} \mathcal{K}(M)$, we set

$$\begin{aligned} \mathcal{D}^-(\mathbf{s}, \mathbf{x}) = &\sum_{N \subseteq L - M} \sum_{\vec{N} \in \Omega(N)} (\mathbf{s} + \Lambda_{\vec{L},\vec{N}}, \Phi^{\vec{N}}_{\mathbf{s}}(\mathbf{x})) \\ \in &\bigoplus_{N \subseteq L - M} \bigoplus_{\vec{N} \in \Omega(N)} \Big(\mathbf{s} + \Lambda_{\vec{L},\vec{N}}, \big(\mathfrak{A}^-(G^{L-M-N}, \psi^{M \cup \vec{N}}(\mathbf{s}))[[\{U_i\}_{L_i \subseteq M \cup N}]]\big) \otimes_{\mathcal{R}} \mathcal{K}(M \cup N) \Big) \\ \subset &\, \mathcal{C}^-(G, \Lambda). \end{aligned}$$

According to Equation (17), $\mathcal{C}^-(G, \Lambda)$ is a chain complex.

Let $H(L,\Lambda) \subseteq \mathbb{Z}^\ell$ be the lattice generated by $\Lambda_i, i = 1,\dots,\ell$. The complex $\mathcal{C}^-(G,\Lambda)$ splits into a direct product of complexes $\mathcal{C}^-(G,\Lambda,\mathfrak{u})$, according to equivalence classes $\mathfrak{u} \in \mathbb{H}(L)/H(L,\Lambda)$. (Note that $H(L,\Lambda)$ is not a subspace of $\mathbb{H}(L)$, but it still acts on $\mathbb{H}(L)$ naturally by addition.) Further, the space of equivalence classes $\mathbb{H}(L)/H(L,\Lambda)$ can be canonically identified with the space of Spin^c structures on the three-manifold $S^3_\Lambda(L)$ obtained from S^3 by surgery along the framed link (L,Λ).

Given a Spin^c structure $\mathfrak{u}$ on $Y_\Lambda(L)$, we set

$$\mathfrak{d}(\mathfrak{u}) = \gcd_{\xi \in H_2(Y_\Lambda(L);\mathbb{Z})} \langle c_1(\mathfrak{u}), \xi\rangle,$$

where $c_1(\mathfrak{u})$ is the first Chern class of the Spin^c structure. Thinking of $\mathfrak{u}$ as an equivalence class in $\mathbb{H}(L)$, we can find a function $\nu : \mathfrak{u} \to \mathbb{Z}/(\mathfrak{d}(\mathfrak{u})\mathbb{Z})$ with the property that

$$\nu(\mathbf{s} + \Lambda_i) \equiv \nu(\mathbf{s}) + 2s_i,$$

for any $i = 1,\dots,\ell$ and $\mathbf{s} = (s_1,\dots,s_\ell) \in \mathfrak{u}$. The function ν is unique up to the addition of a constant. For $\mathbf{s} \in \mathbb{H}(L)$ and $\mathbf{x} \in \big(\mathfrak{A}^-(G^{L-M},\psi^M(\mathbf{s}))[[\{U_i\}_{L_i\subseteq M}]]\big) \otimes_{\mathcal{R}} \mathcal{K}(M)$, let

$$\mu(\mathbf{s},\mathbf{x}) = \mu^M_{\mathbf{s}}(\mathbf{x}) + \nu(\mathbf{s}) - |M|,$$

where $\mu^M_{\mathbf{s}} = \mu_{\psi^M(\mathbf{s})}$ is as in Equation (5), and $|M|$ denotes the number of components of M. Then μ gives a relative $\mathbb{Z}/(\mathfrak{d}(\mathfrak{u})\mathbb{Z})$-grading on the complex $\mathcal{C}^-(G,\Lambda,\mathfrak{u})$. The differential $\mathcal{D}^-$ decreases μ by one modulo $\mathfrak{d}(\mathfrak{u})$.

The following is [12, Theorem 12.7]:

Theorem 2.5. *Fix a grid diagram G with $q \geq 1$ free markings, such that G represents an oriented, ℓ-component link $\vec{L}$ in S^3. Fix also a framing Λ of L. Then, for every $\mathfrak{u} \in \mathrm{Spin}^c(S^3_\Lambda(L))$, we have an isomorphism of relatively graded $\mathbb{F}[[U]]$-modules:*

$$H_*(\mathcal{C}^-(G,\Lambda,\mathfrak{u}),\mathcal{D}^-) \cong \mathbf{HF}^-_*(S^3_\Lambda(L),\mathfrak{u}) \otimes_{\mathbb{F}} H_*(T^{n-q-\ell}), \tag{19}$$

where n is the grid number of G.

Observe that the left hand side of Equation (19) is a priori a module over $\mathcal{R} = \mathbb{F}[[U_1,\dots,U_{\ell+q}]]$. Part of the claim of Theorem 2.5 is that all the U_i's act the same way, so that we have a $\mathbb{F}[[U]]$-module.

2.9. **Maps induced by surgery.** Let $L' \subseteq L$ be a sublink, with the orientation $\vec{L}'$ induced from $\vec{L}$.

Denote by $W = W_\Lambda(L',L)$ the cobordism from $S^3_{\Lambda|_{L'}}(L')$ to $S^3_\Lambda(L)$ given by surgery on $L - L'$, framed with the restriction of Λ. Let $H(L,\Lambda|_{L'}) \subseteq \mathbb{Z}^\ell$ be the sublattice generated by the framings Λ_i, for $L_i \subseteq L'$. There is an identification:

$$\mathrm{Spin}^c(W_\Lambda(L',L)) \cong \mathbb{H}(L)/H(L,\Lambda|_{L'})$$

under which the natural projection

$$\pi^{L,L'} : \big(\mathbb{H}(L)/H(L,\Lambda|_{L'})\big) \longrightarrow \big(\mathbb{H}(L)/H(L,\Lambda)\big)$$

corresponds to restricting the Spin^c structures to $S^3_\Lambda(L)$, while the map

$$\psi^{L-L'} : \big(\mathbb{H}(L)/H(L,\Lambda|_{L'})\big) \to \big(\mathbb{H}(L')/H(L',\Lambda|_{L'})\big)$$

corresponds to restricting them to $S^3_{\Lambda|_{L'}}(L')$.

Observe that, for every equivalence class $\mathbf{t} \in \mathbb{H}(L)/H(L,\Lambda|_{L'})$,

$$\mathcal{C}^-(G,\Lambda)^{L',\mathbf{t}} = \bigoplus_{L-L'\subseteq M\subseteq L} \prod_{\{\mathbf{s}\in\mathbb{H}(L)|[\mathbf{s}]=\mathbf{t}\}} \Big(\mathfrak{A}^-(G^{L-M},\psi^M(\mathbf{s}))[[\{U_i\}_{L_i\subseteq M}]]\Big) \otimes_{\mathcal{R}} \mathcal{K}(M)$$

is a subcomplex of $\mathcal{C}^-(G,\Lambda,\pi^{L,L'}(\mathbf{t})) \subseteq \mathcal{C}^-(G,\Lambda)$. This subcomplex is chain homotopy equivalent to

$$\mathcal{C}^-(G^{L'},\Lambda|_{L'},\psi^{L-L'}(\mathbf{t})) \otimes H_*(T^{(n-n')-(\ell-\ell')}),$$

where

$$\mathcal{C}^-(G^{L'}, \Lambda|_{L'}, \psi^{L-L'}(\mathbf{t})) = \bigoplus_{M'\subseteq L'} \prod_{\{\mathbf{s}'\in\mathbb{H}(L')|[\mathbf{s}']=\psi^{L-L'}(\mathbf{t})\}} \Big(\mathfrak{A}^-(G^{L'-M'}, \psi^{M'}(\mathbf{s}'))[[\{U_i\}_{L_i\subseteq M'}]]\Big) \otimes_{\mathcal{R}'} \mathcal{K}(M')$$

and $\mathcal{R}'$ is the power series ring in the U_i variables from L'. The chain homotopy equivalence is induced by taking M to $M' = M-(L-L')$, $\mathbf{s}$ to $\mathbf{s}' = \psi^{\vec{L}-\vec{L}'}(\mathbf{s})$, and getting rid of the U_i variables from $L-L'$ via relations coming from $\mathcal{K}(L-L')$.

Theorem 2.5 implies that the homology of $\mathcal{C}^-(G,\Lambda)^{L',\mathbf{t}}$ is isomorphic to

$$\mathbf{HF}^-_*(S^3_{\Lambda'}(L'), \mathbf{t}|_{S^3_{\Lambda|_{L'}}(L')}) \otimes H_*(T^{n-q-\ell}).$$

In [24], Ozsváth and Szabó associated a map $F^-_{W,\mathbf{s}}$ to any cobordism W between connected three-manifolds, and Spin^c structure $\mathbf{t}$ on that cobordism. In the case when the cobordism W consists only of two-handles (i.e., is given by integral surgery on a link), the following theorem gives a way of understanding the map $F^-_{W,\mathbf{t}}$ in terms of grid diagrams:

Theorem 2.6. *Let $\vec{L} \subset S^3$ be an ℓ-component link, $L' \subseteq L$ a sublink, G a grid diagram for $\vec{L}$ of grid number n and having $q \geq 1$ free markings, and Λ a framing of L. Set $W = W_\Lambda(L', L)$. Then, for any $\mathbf{t} \in \mathrm{Spin}^c(W) \cong \mathbb{H}(L)/H(L, \Lambda|_{L'})$, the following diagram commutes:*

$$\begin{tikzcd}
H_*(\mathcal{C}^-(G,\Lambda)^{L',\mathbf{t}}) \arrow[r] \arrow[d, "\cong"'] & H_*(\mathcal{C}^-(G,\Lambda,\pi^{L,L'}(\mathbf{t}))) \arrow[d, "\cong"] \\
\mathbf{HF}^-_*(S^3_{\Lambda'}(L'), \mathbf{t}|_{S^3_{\Lambda|_{L'}}(L')}) \otimes H_*(T^{n-q-\ell}) \arrow[r, "F^-_{W,\mathbf{t}}\otimes \mathrm{Id}"] & \mathbf{HF}^-_*(S^3_\Lambda(L), \mathbf{t}|_{S^3_{\Lambda|_L}(L)}) \otimes H_*(T^{n-q-\ell}).
\end{tikzcd}$$

Here, the top horizontal map is induced from the inclusion of chain complexes, while the two vertical isomorphisms are the ones from Theorem 2.5.

Theorem 2.6 is basically [12, Theorem 11.1], but stated here in the particular setting of grid diagrams. See [12, Remark 12.8].

2.10. **Other versions.** The chain complex $\mathcal{C}^-(G,\Lambda,\mathfrak{u})$ was constructed so that the version of Heegaard Floer homology appearing in Theorem 2.5 is $\mathbf{HF}^-$. We now explain how one can construct similar chain complexes $\hat{\mathcal{C}}(G,\Lambda,\mathfrak{u}), \mathcal{C}^+(G,\Lambda,\mathfrak{u})$ and $\mathcal{C}^\infty(G,\Lambda,\mathfrak{u})$, corresponding to the theories $\widehat{HF}$, HF^+ and $\mathbf{HF}^\infty$.

The chain complex $\hat{\mathcal{C}}(G,\Lambda,\mathfrak{u})$ is simply obtained from $\mathcal{C}^-(G,\Lambda)$ by setting one of the variables U_i equal to zero. Its homology computes $\widehat{HF}(S^3_\Lambda(L),\mathfrak{u}) \otimes H^*(T^{n-q-\ell})$.

The chain complex $\mathcal{C}^\infty(G,\Lambda,\mathfrak{u})$ is obtained from $\mathcal{C}^-(G,\Lambda,\mathfrak{u})$ by inverting all the U_i variables. It is a vector space over the field of semi-infinite Laurent polynomials

$$\mathcal{R}^\infty = \mathbb{F}[[U_1,\dots,U_{\ell+q}; U_1^{-1},\dots,U_{\ell+q}^{-1}].$$

In other words, $\mathcal{R}^\infty$ consists of those power series in U_i's that are sums of monomials with degrees bounded from below.

Note that $C^-(G,\Lambda,\mathfrak{u})$ is a subcomplex of $\mathcal{C}^\infty(G,\Lambda,\mathfrak{u})$. We denote the quotient complex by $\mathcal{C}^+(G,\Lambda,\mathfrak{u})$. Theorems 2.5 and 2.6 admit the following extension:

Theorem 2.7. *Fix a grid diagram G (of grid number n, and with $q \geq 1$ free markings) for an oriented, ℓ-component link $\vec{L}$ in S^3, and fix a framing Λ of L. Choose also an ordering of the components of $\vec{L}$, as well as of the O and X markings on the grid G. Set $V = H_*(T^{n-q-\ell})$. Then,*

for every $\mathfrak{u} \in \mathrm{Spin}^c(S^3_\Lambda(L)) \cong \mathbb{H}(L)/H(L,\Lambda)$, *there are vertical isomorphisms and horizontal long exact sequences making the following diagram commute:*

$$\begin{tikzcd}
\cdots \to H_*(\mathcal{C}^-(G,\Lambda,\mathfrak{u})) \arrow[r] \arrow[d, "\cong"] & H_*(\mathcal{C}^\infty(G,\Lambda,\mathfrak{u})) \arrow[r] \arrow[d, "\cong"] & H_*(\mathcal{C}^+(G,\Lambda,\mathfrak{u})) \to \cdots \arrow[d, "\cong"] \\
\cdots \to \mathbf{HF}^-_*(S^3_\Lambda(L),\mathfrak{u}) \otimes V \arrow[r] & \mathbf{HF}^\infty_*(S^3_\Lambda(L),\mathfrak{u}) \otimes V \arrow[r] & HF^+_*(S^3_\Lambda(L),\mathfrak{u}) \otimes V \to \cdots
\end{tikzcd}$$

Furthermore, the maps in these diagrams behave naturally with respect to cobordisms, in the sense that there are commutative diagrams analogous to those in Theorem 2.6, involving the cobordism maps $F^-_{W,\mathfrak{t}}, F^\infty_{W,\mathfrak{t}}, F^+_{W,\mathfrak{t}}$.

Compare [12, Theorem 11.2].

2.11. **Mixed invariants of closed four-manifolds.** We recall the definition of the closed four-manifold invariant from [24]. Let X be a closed, oriented four-manifold with $b_2^+(X) \geq 2$. By puncturing X in two points we obtain a cobordism W from S^3 to S^3. We can cut W along a three-manifold N so as to obtain two cobordisms W_1, W_2 with $b_2^+(W_i) > 0$; further, the manifold N can be chosen such that $\delta H^1(N;\mathbb{Z}) \subset H^2(W;\mathbb{Z})$ is trivial. (If this is the case, N is called an *admissible cut.*) Let $\mathfrak{t}$ be a Spin^c structure on X and $\mathfrak{t}_1, \mathfrak{t}_2$ its restrictions to W_1, W_2. In this situation, the cobordism maps

$$F^-_{W_1,\mathfrak{t}_1} : \mathbf{HF}^-(S^3) \to \mathbf{HF}^-(N, \mathfrak{t}|_N)$$

and

$$F^+_{W_2,\mathfrak{t}_2} : HF^+(N,\mathfrak{t}|_N) \to HF^+(S^3)$$

factor through $HF_{\mathrm{red}}(N,\mathfrak{t}|_N)$, where

$$HF_{\mathrm{red}} = \mathrm{Coker}(\mathbf{HF}^\infty \to HF^+) \cong \mathrm{Ker}(\mathbf{HF}^- \to \mathbf{HF}^\infty).$$

By composing the maps to and from HF_{red} we obtain the mixed map

$$F^{\mathrm{mix}}_{W,\mathfrak{t}} : \mathbf{HF}^-(S^3) \to HF^+(S^3),$$

which changes degree by the quantity

$$d(\mathfrak{t}) = \frac{c_1(\mathfrak{t})^2 - 2\chi(X) - 3\sigma(X)}{4}.$$

Let Θ_- be the maximal degree generator in $\mathbf{HF}^-(S^3)$. Clearly the map $F^{\mathrm{mix}}_{W,\mathfrak{t}}$ can be nonzero only when $d(\mathfrak{t})$ is even and nonnegative. If this is the case, the value

$$\Phi_{X,\mathfrak{t}} = U^{d(\mathfrak{t})/2} \cdot F^{\mathrm{mix}}_{W,\mathfrak{t}}(\Theta_-) \in HF^+_0(S^3) \cong \mathbb{F} \tag{20}$$

is an invariant of the four-manifold X and the Spin^c structure $\mathfrak{t}$. It is conjecturally the same as the Seiberg-Witten invariant of $(X,\mathfrak{t})$.

Definition 2.8. *Let X be a closed, oriented four-manifold with $b_2^+(X) \geq 2$. A* cut link presentation *for X consists of a link $L \subset S^3$, a decomposition of L as a disjoint union*

$$L = L_1 \amalg L_2 \amalg L_3,$$

and a framing Λ for L (with restrictions Λ_i to $L_i, i = 1, \dots, 4$) with the following properties:

- $S^3_{\Lambda_1}(L_1)$ *is a connected sum of m copies of $S^1 \times S^2$, for some $m \geq 0$. We denote by W_1 the cobordism from S^3 to $\#^m(S^1 \times S^2)$ given by m one-handle attachments.*
- $S^3_{\Lambda_1 \cup \Lambda_2 \cup \Lambda_3}(L_1 \cup L_2 \cup L_3)$ *is a connected sum of m' copies of $S^1 \times S^2$, for some $m' \geq 0$. We denote by W_4 the cobordism from $\#^{m'}(S^1 \times S^2)$ to S^3 given by m' three-handle attachments.*

- *If we denote by* W_2 *resp.* W_3 *the cobordisms from* $S^3_{\Lambda_1}(L_1)$ *to* $S^3_{\Lambda_1\cup\Lambda_2}(L_1\cup L_2)$*, resp. from* $S^3_{\Lambda_1\cup\Lambda_2}(L_1\cup L_2)$ *to* $S^3_{\Lambda_1\cup\Lambda_2\cup\Lambda_3}(L_1\cup L_2\cup L_3)$*, given by surgery on* L_2 *resp.* L_3 *(i.e., consisting of two-handle additions), then*
$$W = W_1 \cup W_2 \cup W_3 \cup W_4$$
is the cobordism from S^3 *to* S^3 *obtained from* X *by deleting two copies of* B^4*.*
- *The manifold* $N = S^3_{\Lambda_1\cup\Lambda_2}(L_1\cup L_2)$ *is an admissible cut for* W*, i.e.,* $b_2^+(W_1\cup W_2) > 0, b_2^+(W_3\cup W_4) > 0$*, and* $\delta H^1(N) = 0$ *in* $H^2(W)$*.*

It is proved in [12, Lemma 8.7] that any closed, oriented four-manifold X with $b_2^+(X)\geq 2$ admits a cut link presentation.

Definition 2.9. *Let* X *be a closed, oriented four-manifold with* $b_2^+(X)\geq 2$*. A* grid presentation Γ *for* X *consists of a cut link presentation* $(L = L_1\cup L_2\cup L_3, \Lambda)$ *for* X*, together with a grid presentation for* L*.*

The four-manifold invariant $\Phi_{X,\mathfrak{t}}$ can be expressed in terms of a grid presentation Γ for X as follows. By combining the maps $F^-_{W_2,\mathfrak{t}|_{W_2}}$ and $F^+_{W_3,\mathfrak{t}|_{W_3}}$ using their factorization through HF_{red}, we obtain a mixed map
$$F^{\mathrm{mix}}_{W_2\cup W_3,\mathfrak{t}|_{W_2\cup W_3}} : \mathbf{HF}^-(\#^m(S^1\times S^2)) \to HF^+(\#^{m'}(S^1\times S^2)).$$

Using Theorem 2.7, we can express the maps $F^-_{W_2,\mathfrak{t}|_{W_2}}$ and $F^+_{W_3,\mathfrak{t}|_{W_3}}$ (or, more precisely, their tensor product with the identity on $V = H_*(T^{n-\ell})$) in terms of counts of holomorphic polygons on a symmetric product of the grid. Combining these polygon counts, we get a mixed map
$$F^{\mathrm{mix}}_{\Gamma,\mathfrak{t}} : H_*(\mathcal{C}^-(G,\Lambda)^{L_1,\mathfrak{t}|_{W_2\cup W_3}}) \to H_*(\mathcal{C}^+(G,\Lambda)^{L_1\cup L_2\cup L_3,\mathfrak{t}|_{\#^{m'}(S^1\times S^2)}}).$$
We conclude that $F^{\mathrm{mix}}_{\Gamma,\mathfrak{t}}$ is the same as $F^{\mathrm{mix}}_{W_2\cup W_3,\mathfrak{t}|_{W_2\cup W_3}}\otimes \mathrm{Id}_V$, up to compositions with isomorphisms on both the domain and the target. Note, however, that at this point we do not know how to identify elements in the domains (or targets) of the two maps in a canonical way. For example, we know that there is an isomorphism
$$H_*(\mathcal{C}^-(G,\Lambda)^{L_1,\mathfrak{t}|_{W_2\cup W_3}}) \cong \mathbf{HF}^-(\#^m(S^1\times S^2))\otimes V, \tag{21}$$
but it is difficult to say exactly what the isomorphism is. Nevertheless, both $\mathbf{HF}^-(\#^m(S^1\times S^2))$ and V have unique maximal degree elements Θ^m_{max} and Θ_V, respectively. We can identify what $\Theta^m_{\mathrm{max}}\otimes\Theta_V$ corresponds to on the left hand side of (21) by simply computing degrees. Let us denote the respective element by
$$\Theta^\Gamma_{\mathrm{max}} \in H_*(\mathcal{C}^-(G,\Lambda)^{L_1,\mathfrak{t}|_{W_2\cup W_3}}).$$

The following proposition says that one can decide whether $\Phi_{X,\mathfrak{t}}\in\mathbb{F}$ is zero or one from information coming from a grid presentation Γ:

Proposition 2.10. *Let* X *be a closed, oriented four-manifold* X *with* $b_2^+(X)\geq 2$*, with a* Spin^c *structure* $\mathfrak{t}$ *with* $d(\mathfrak{t})\geq 0$ *even. Let* Γ *be a grid presentation for* X*. Then* $\Phi_{X,\mathfrak{t}} = 1$ *if and only if* $U^{d(\mathfrak{t})/2}\cdot F^{\mathrm{mix}}_{\Gamma,\mathfrak{t}}(\Theta^\Gamma_{\mathrm{max}})$ *is nonzero.*

Compare [12, Theorem 11.7].

2.12. **The link surgeries spectral sequence.** We recall the construction from [23, Section 4]. Let $M = M_1\cup\cdots\cup M_\ell$ be a framed ℓ-component link in a 3-manifold Y. For each $\varepsilon = (\varepsilon_1,\dots,\varepsilon_\ell)\in\mathbb{E}_\ell = \{0,1\}^\ell$, we let $Y(\varepsilon)$ be the 3-manifold obtained from Y by doing ε_i-framed surgery on M_i for $i = 1,\dots,\ell$.

When ε' is an immediate successor to ε (that is, when $\varepsilon < \varepsilon'$ and $\|\varepsilon' - \varepsilon\| = 1$), the two-handle addition from $Y(\varepsilon)$ to $Y(\varepsilon')$ induces a map on Heegaard Floer homology

$$F^-_{\varepsilon<\varepsilon'} : \mathbf{HF}^-(Y(\varepsilon)) \longrightarrow \mathbf{HF}^-(Y(\varepsilon')).$$

The following is the link surgery spectral sequence (Theorem 4.1 in [23], but phrased here in terms of $\mathbf{HF}^-$ rather than $\widehat{HF}$ or HF^+):

Theorem 2.11 (Ozsváth-Szabó)**.** *There is a spectral sequence whose E^1 term is $\bigoplus_{\varepsilon \in \mathbb{E}_\ell} \mathbf{HF}^-(Y(\varepsilon))$, whose d_1 differential is obtained by adding the maps $F^-_{\varepsilon<\varepsilon'}$ (for ε' an immediate successor of ε), and which converges to $E^\infty \cong \mathbf{HF}^-(Y)$.*

Remark 2.12. A special case of Theorem 2.11 gives a spectral sequence relating the Khovanov homology of a link and the Heegaard Floer homology of its branched double cover. See [23, Theorem 1.1].

The spectral sequence in Theorem 2.11 can be understood in terms of grid diagrams as follows.

We represent $Y(0, \dots, 0)$ itself as surgery on a framed link (L', Λ') inside S^3. Let $L'_1, \dots, L'_{\ell'}$ be the components of L'. There is another framed link $(L = L_1 \cup \dots \cup L_\ell, \Lambda)$ in S^3, disjoint from L', such that surgery on each component L_i (with the given framing) corresponds exactly to the 2-handle addition from $Y(0, \dots, 0)$ to $Y(0, \dots, 0, 1, 0, \dots, 0)$, where the 1 is in position i. For $\varepsilon \in \mathbb{E}_\ell$, we denote by L^ε the sublink of L consisting of those components L_i such that $\varepsilon_i = 1$.

Let G be a toroidal grid diagram representing the link $L' \cup L \subset S^3$. As mentioned in Section 2.9, inside the surgery complex $\mathcal{C}^-(G, \Lambda' \cup \Lambda)$ (which is an $(\ell' + \ell)$-dimensional hypercube of chain complexes) we have various subcomplexes which compute the Heegaard Floer homology of surgery on the sublinks on $L' \cup L$. We will restrict our attention to those sublinks that contain L', and use the respective subcomplexes to construct a new, ℓ-dimensional hypercube of chain complexes $\mathcal{C}^-(G, \Lambda' \cup \Lambda /\!\!/ L)$ as follows.

At a vertex $\varepsilon \in \mathbb{E}_\ell$ we put the complex

$$\mathcal{C}^-(G, \Lambda' \cup \Lambda /\!\!/ L)^\varepsilon = \mathcal{C}^-(G^{L' \cup L^\varepsilon}, \Lambda' \cup \Lambda|_{L^\varepsilon}) \otimes H_*(T^{(n-n_\varepsilon)-(\ell-\|\varepsilon\|)}),$$

where n_ε is the size of the grid diagram $G^{L' \cup L^\varepsilon}$.

Consider now an edge from ε to $\varepsilon' = \varepsilon + \tau_i$ in the hypercube $\mathbb{E}_\ell$. The corresponding complex $\mathcal{C}^-(G^{L' \cup L^\varepsilon}, \Lambda' \cup \Lambda|_{L^\varepsilon})$ decomposes as a direct product over all Spin^c structures $\mathbf{s}$ on $Y(\varepsilon) = S^3(L' \cup L^\varepsilon, \Lambda' \cup \Lambda|_{L^\varepsilon})$. As explained in Section 2.9, each factor $\mathcal{C}^-(G^{L' \cup L^\varepsilon}, \Lambda' \cup \Lambda|_{L^\varepsilon}, \mathbf{s})$ (tensored with the appropriate homology of a torus) admits an inclusion into $\mathcal{C}^-(G^{L' \cup L^{\varepsilon'}}, \Lambda' \cup \Lambda|_{L^{\varepsilon'}})$ as a subcomplex. In fact, there are several such inclusion maps, one for each Spin^c structure $\mathbf{t}$ on the 2-handle cobordism from $Y(\varepsilon)$ to $Y(\varepsilon')$ such that $\mathbf{t}$ restricts to $\mathbf{s}$ on $Y(\varepsilon)$. Adding up all the inclusion maps on each factor, one obtains a combined map

$$G^-_{\varepsilon<\varepsilon'} : \mathcal{C}^-(G, \Lambda' \cup \Lambda /\!\!/ L)^\varepsilon \longrightarrow \mathcal{C}^-(G, \Lambda' \cup \Lambda /\!\!/ L)^{\varepsilon'}.$$

We take $G^-_{\varepsilon<\varepsilon'}$ to be the edge map in the hypercube of chain complexes $\mathcal{C}^-(G, \Lambda' \cup \Lambda /\!\!/ L)$. Since the edge maps are just sums of inclusions of subcomplexes, they commute on the nose along each face of the hypercube. Therefore, in the hypercube $\mathcal{C}^-(G, \Lambda' \cup \Lambda /\!\!/ L)$ we can take the diagonal maps to be zero, along all faces of dimension at least two.

This completes the construction of $\mathcal{C}^-(G, \Lambda' \cup \Lambda /\!\!/ L)$. As an ℓ-dimensional hypercube of chain complexes, its total complex admits a filtration by $-\|\varepsilon\|$, which induces a spectral sequence; we refer to the filtration by $-\|\varepsilon\|$ as the *depth filtration* on $\mathcal{C}^-(G, \Lambda' \cup \Lambda /\!\!/ L)$.

The following is [12, Theorem 11.9], adapted here to the setting of grid diagrams:

Theorem 2.13. *Fix a grid diagram G with $q \geq 1$ free markings, such that G represents an oriented link $\vec{L}' \cup \vec{L}$ in S^3. Fix also framings Λ for L and Λ' for L'. Suppose G has grid number n, and that L has ℓ components $L_1, \dots, L_\ell$. Let $Y(0, \dots, 0) = S^3_{\Lambda'}(L')$, and let $Y(\varepsilon)$ be obtained from $Y(0, \dots, 0)$ by surgery on the components $L_i \subseteq L$ with $\varepsilon_i = 1$ (for any $\varepsilon \in \mathbb{E}_\ell$). Then, there is an isomorphism*

between the link surgeries spectral sequence from Theorem 2.11, tensored with $V = H_*(T^{n-q-\ell})$, and the spectral sequence associated to the depth filtration on $\mathcal{C}^-(G, \Lambda' \cup \Lambda /\!\!/ L)$.

3. Enhanced domains of holomorphic polygons

3.1. **Domains and shadows.** In the construction of the complex $\mathcal{C}^-(G,\Lambda)$ in Section 2.8, the only non-combinatorial ingredients were the holomorphic polygon counts in the definition of the maps $D^{\mathcal{Z}}_{\mathbf{s}}$. (We use here the notation from Remark 2.3.) According to Equation (8), the maps $D^{\mathcal{Z}}_{\mathbf{s}}$ are in turn summations of maps of the form $D^{(\mathcal{Z})}_{\mathbf{s}}$, where $(\mathcal{Z})$ denotes an ordering of a consistent collection of markings $\mathcal{Z}$.

Let $(\mathcal{Z}) = (Z_1, \dots, Z_k)$. The maps

$$D^{(\mathcal{Z})}_{\mathbf{s}} : \mathfrak{A}^-(\mathbb{T}_\alpha, \mathbb{T}^{\mathcal{Z}^0}_\beta, \mathbf{s}) \to \mathfrak{A}^-(\mathbb{T}_\alpha, \mathbb{T}^{\mathcal{Z}^0 \cup \mathcal{Z}}_\beta, \mathbf{s}),$$

correspond to destabilization (in the given order) at a set of markings $\mathcal{Z}$, starting with a diagram G already destabilized at a base set of markings $\mathcal{Z}^0$. Our goal is to get as close as possible to a combinatorial description of these maps. In light of the isomorphisms (11), we can assume without loss of generality that $\mathcal{Z}_0 = \emptyset$. The difficulty lies in understanding the counts of pseudo-holomorphic polygons $\#\mathcal{M}(\phi)$, where

$$\phi \in \pi_2(\mathbf{x}, \Theta^{\emptyset,\{Z_1\}}, \Theta^{\{Z_1\},\{Z_1,Z_2\}}, \dots, \Theta^{\{Z_1,\dots,Z_{k-1}\},\{Z_1,\dots,Z_k\}}, \mathbf{y})$$

is a homotopy class of $(2+k)$-gons with edges on

$$\mathbb{T}_\alpha, \mathbb{T}_\beta, \mathbb{T}^{\{Z_1\}}_\beta, \mathbb{T}^{\{Z_1,Z_2\}}_\beta, \dots, \mathbb{T}^{\{Z_1,\dots,Z_k\}}_\beta,$$

in this cyclic order. The Maslov index $\mu(\phi)$ is required to be $1-k$.

As in [22, Definition 2.13], every homotopy class ϕ has an associated *domain* $D(\phi)$ on the surface $\mathcal{T}$. The domain is a linear combination of regions, i.e., connected components of the complement in $\mathcal{T}$ of all the curves $\alpha, \beta, \beta^{\{Z_1\}}, \beta^{\{Z_1,Z_2\}}, \dots, \beta^{\{Z_1,\dots,Z_k\}}$. If ϕ admits a holomorphic representative, then $D(\phi)$ is a linear combination of regions, all appearing with nonnegative coefficients.

Let us mark an asterisk in each square of the grid diagram G. When we construct the new beta curves $\beta^{\{Z_1\}}, \beta^{\{Z_1,Z_2\}}, \dots, \beta^{\{Z_1,\dots,Z_k\}}$ (all obtained from the original β curves by handleslides), we make sure that each beta curve encircling a marking does not include an asterisk, and also that whenever we isotope a beta curve to obtain a new beta curve intersecting it in two points, these isotopies do not cross the asterisks. Then the regions on $\mathcal{T}$ fall naturally into two types: *small* regions, which do not contain asterisks, and *large* regions, which do. We define the *shadow* $Sh(R)$ of a large region R to be the square in G containing the same asterisk as R; and the shadow of a small region to be the empty set.

If

$$D = \sum a_i R_i$$

is a linear combination of regions, with $a_i \in \mathbb{Z}$, we define its shadow to be

$$Sh(D) = \sum a_i Sh(R_i).$$

The *shadow* $Sh(\phi)$ of a homotopy class ϕ is defined as $Sh(D(\phi))$. See Figure 5.

We will study homotopy classes ϕ by looking at their shadows, together with two additional pieces of data as follows.

First, each homotopy class ϕ corresponds to a $(2+k)$-gon where one vertex is an intersection point $\mathbf{y} \in \mathbb{T}_\alpha \cap \mathbb{T}^{\mathcal{Z}}_\beta$. In particular, $\mathbf{y}$ contains exactly one of the two intersection points between the alpha curve just below the marking Z_i and the beta curve encircling Z_i, for $i = 1, \dots, k$. Set $\epsilon_i = 0$ if that point is the left one, and $\epsilon_j = 1$ if it is the right one.

Second, for $i = 1, \dots, k$, let $\rho_i \in \mathbb{Z}$ be the multiplicity of the domain $D(\phi)$ at the marking Z_i.

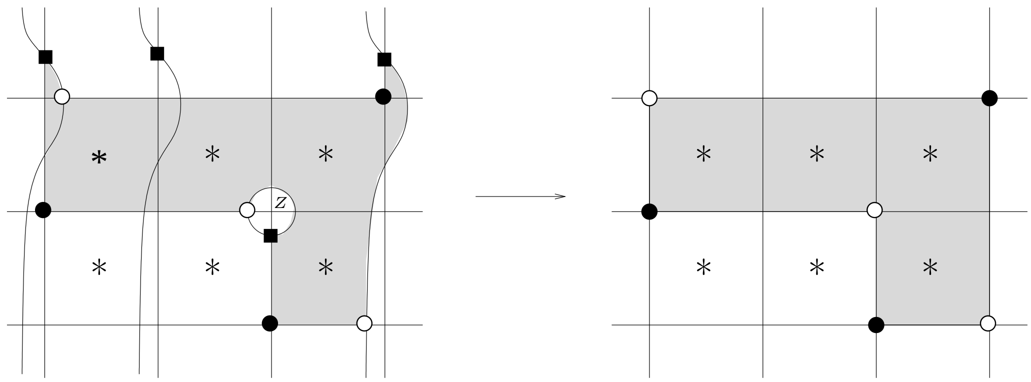

Figure 5. **The domain of a triangle and its shadow.** On the left, we show the domain $D(\phi)$ of a homotopy class ϕ of triangles in $\mathrm{Sym}^n(\mathcal{T})$. The alpha and beta curves are the horizontal and vertical straight lines, respectively, while the curved arcs (including the one encircling Z) are part of the $\beta^{\{Z\}}$ curves. The black squares mark components of $\Theta^{\emptyset,\{Z\}} \in \mathbb{T}_\beta \cap \mathbb{T}_\beta^{\{Z\}}$. On the right, we show the shadow $Sh(\phi)$.

Then, we define the *enhanced domain* $E(\phi)$ associated to ϕ to be the triple $(Sh(\phi), \epsilon(\phi), \rho(\phi))$ consisting of the shadow $Sh(\phi)$, the collection $\epsilon(\phi) = (\epsilon_1, \dots, \epsilon_k)$ corresponding to $\mathbf{y}$, and the set of multiplicities $\rho(\phi) = (\rho_1, \dots, \rho_k)$.

3.2. **Grid diagrams marked for destabilization.** We now turn to studying enhanced domains on their own. For simplicity, we will assume that all the markings $Z_1, \dots, Z_k$ relevant for our destabilization procedure are O's. (The set of allowable domains will be described by the same procedure if some markings are X's.)

Consider a toroidal grid diagram G of grid number n. We ignore the X's, and consider the n O's with associated variables $U_1, \dots, U_n$. Note that, unlike in Section 2.2, here we use one variable for each O, rather than one for each link component.

Some subset

$$\mathcal{Z} = \{O_{i_1}, \dots, O_{i_k}\}$$

of the O's, corresponding to indices $i_1, \dots, i_k \in \{1, \dots, n\}$, is marked for destabilization. (These are the markings $Z_1, \dots, Z_k$ from the previous subsection.) We will assume that $k < n$. (This is always the case in our setting, when we start with at lest one free basepoint.) The corresponding points on the lower left of each O_{i_j} are denoted p_j and called *destabilization points.*

Let $C^-(G) = \mathbf{CF}^-(\mathbb{T}_\alpha, \mathbb{T}_\beta)$ be the chain complex freely generated over $\mathbb{F}[[U_1, \dots, U_n]]$ by the $n!$ elements of $\mathbf{S}(G)$, namely the n-tuples of intersection points on the grid. Its differential ∂ counts rectangles, while keeping track of the U's:

$$\partial^- \mathbf{x} = \sum_{\mathbf{y} \in \mathbf{S}(G)} \sum_{r \in \mathrm{Rect}^\circ(\mathbf{x},\mathbf{y})} U_1^{O_1(r)} \cdots U_n^{O_n(r)} \mathbf{y}.$$

Each generator $\mathbf{x} \in \mathbf{S}(G)$ has a well-defined homological grading $M(\mathbf{x}) \in \mathbb{Z}$. Note that $M(U_i \cdot \mathbf{x}) = M(\mathbf{x}) - 2$.

Let $G^{\mathcal{Z}}$ be the destabilized diagram. There is a similar complex $C^-(G^{\mathcal{Z}})$. We identify $\mathbf{S}(G^{\mathcal{Z}})$ with a subset of $\mathbf{S}(G)$ by adjoining to an element of $\mathbf{S}(G^{\mathcal{Z}})$ the destabilization points.

The set of *enhanced generators* $\mathbf{ES}(G, \mathcal{Z})$ consists of pairs $(\mathbf{y}, \epsilon)$, where $\mathbf{y} \in \mathbf{S}(G^{\mathcal{Z}})$ and $\epsilon = (\epsilon_1, \dots, \epsilon_k)$ is a collection of markings ($\epsilon_j = 0$ or 1) at each destabilization point. We will also denote these markings as L for a left marking ($\epsilon_j = 0$) or R for a right marking ($\epsilon_j = 1$). The

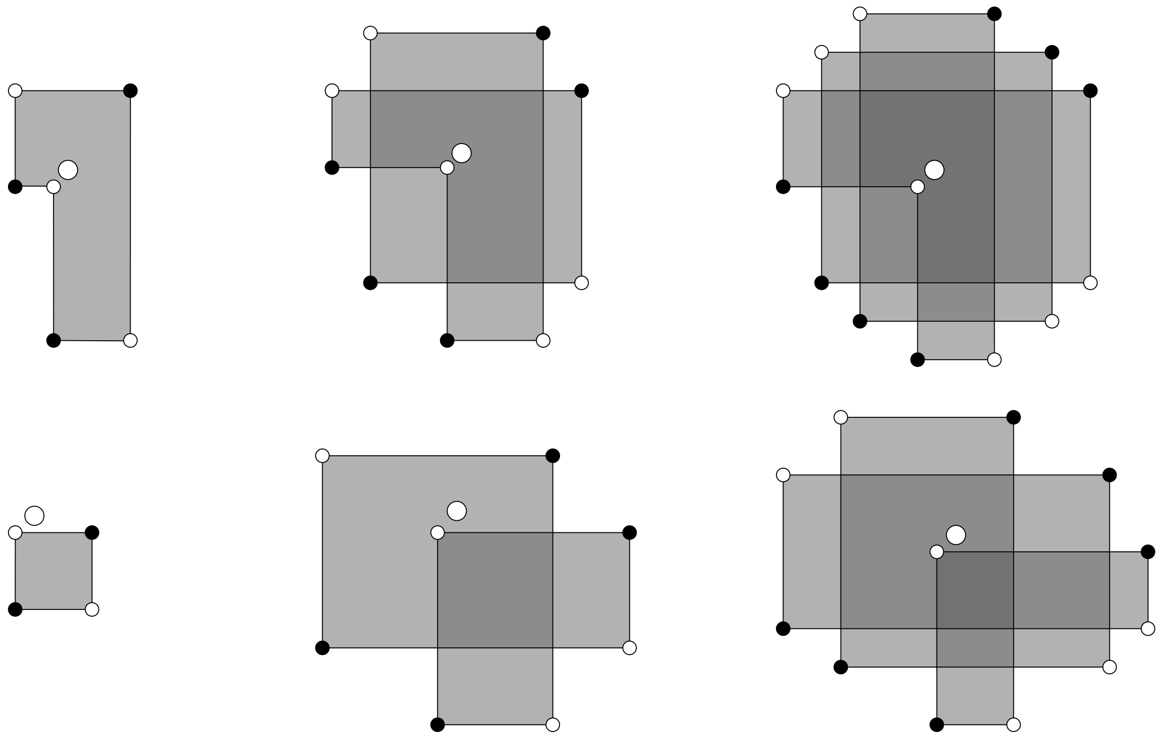

FIGURE 6. **Domains for destabilization at one point.** We label initial points by dark circles, and terminal points by empty circles. The top row lists domains of type L (i.e., ending in an enhanced generator with an L marking), while the second row lists some of type R. Darker shading corresponds to higher local multiplicities. The domains in each row (top or bottom) are part of an infinite series, corresponding to increasing complexities. The series in the first row also contains the trivial domain of type L, not shown here.

homological grading of an enhanced generator is

$$M(\mathbf{y}, \epsilon) = M(\mathbf{y}) + \sum_{j=1}^{k} \epsilon_j.$$

We define an enhanced destabilized complex $EC^-(G, \mathcal{Z})$ whose generators are $\mathbf{ES}(G, \mathcal{Z})$. It is formed as the tensor product of k mapping cones

$$C^-(G^{\mathcal{Z}}) \to C^-(G^{\mathcal{Z}}) \tag{22}$$

given by the map $U_{i_j} - U_{i'_j}$ from L to R, where $U_{i'_j}$ corresponds to the O in the row directly below the destabilization point p_j. For a suitable choice of almost-complex structure on the symmetric product, there is a natural isomorphism

$$EC^-(G, \mathcal{Z}) \cong \mathbf{CF}^-(\mathbb{T}_\alpha, \mathbb{T}_\beta^{\{O_{i_1}, \dots, O_{i_k}\}}),$$

with the caveat that on the right hand side we count different U variables than we did in Section 2.4.

It was shown in [14, Section 3.2] that in the case $k = 1$ there is a quasi-isomorphism

$$F : C^-(G) \to EC^-(G, \mathcal{Z}) \tag{23}$$

given by counting snail-like domains as in Figure 6.

Definition 3.1. *Given a domain D on the α-β grid (that is, a linear combination of squares), we let $O_i(D)$ be the multiplicity of D at O_i. We define an* enhanced domain (D, ϵ, ρ) *to consists of:*

- *A domain D on the grid between points $\mathbf{x} \in \mathbf{S}(G)$ and $\mathbf{y} \in \mathbf{S}(G^{\mathcal{Z}})$ (in particular, the final configuration contains all destabilization points);*
- *A set of markings $\epsilon = (\epsilon_1, \dots, \epsilon_k)$ at each destabilization point (so that $(\mathbf{y}, \epsilon)$ is an enhanced generator); and*
- *A set of integers $\rho = (\rho_1, \dots, \rho_k)$, one for each destabilization point.*

We call ρ_j the *real multiplicity* at O_{i_j}. The number $t_j = O_{i_j}(D)$ is called the *total multiplicity*, and the quantity $f_j = t_j - \rho_j$ is called the *fake multiplicity* at O_{i_j}. The reason for this terminology is that, if D is the shadow of a holomorphic $(k+2)$-gon D', then the real multiplicity ρ_j is the multiplicity of D' at O_{i_j}. On the other hand, the fake multiplicity (if positive) is the multiplicity that appears in the shadow even though it does not come from the polygon. For example, in the domain pictured in Figure 5, the fake multiplicity at the Z marking is one.

Consider the full collection of real multiplicities $(N_1, \dots, N_n)$, where $N_{i_j} = \rho_j$ for $j \in \{1, \dots, k\}$, and $N_i = O_i(D)$ when O_i is not one of the O's used for destabilization. We say that the enhanced domain (D, ϵ, ρ) goes from the generator $\mathbf{x}$ to $U_1^{N_1} \cdots U_n^{N_n} \cdot (\mathbf{y}, \epsilon)$. These are called the initial and final point of the enhanced domain, respectively.

We define the *index* of an enhanced domain to be

$$\begin{aligned} I(D, \epsilon, \rho) &= M(\mathbf{x}) - M(U_1^{N_1} \cdots U_n^{N_n} \cdot (\mathbf{y}, \epsilon)) \\ &= M(\mathbf{x}) - M(\mathbf{y}) - \sum_{j=1}^{k} \epsilon_j + 2 \sum_{j=1}^{k} N_i \\ &= M(\mathbf{x}) - M(U_1^{O_1(D)} \cdots U_n^{O_n(D)} \cdot \mathbf{y}) - \sum_{j=1}^{k} (\epsilon_j + 2 f_j) \\ &= I(D) - \sum_{j=1}^{k} (\epsilon_j + 2 f_j). \end{aligned} \tag{24}$$

Here $I(D)$ is the ordinary Maslov index of D, given by Lipshitz's formula [7, Corollary 4.3]:

$$I(D) = \sum_{x \in \mathbf{x}} n_x(D) + \sum_{y \in \mathbf{y}} n_y(D), \tag{25}$$

where $n_p(D)$ denotes the average multiplicity of D in the four quadrants around the point p. (Lipshitz's formula in the reference has an extra term, the Euler measure of D, but this is zero in our case because D can be decomposed into rectangles.)

For example, consider the domains in Figure 6. We turn them into enhanced domains by adding the respective marking (L or R) as well as choosing the real multiplicity at the destabilization point to be zero. Then all those domains have index zero, regardless of how many (non-destabilized) O's they contain and with what multiplicities.

Lemma 3.2. *Suppose that (D, ϵ, ρ) is the enhanced domain associated to a homotopy class ϕ of $(k+2)$-gons as in Section 3.2. Then the Maslov indices match: $\mu(\phi) = I(D, \epsilon, \rho)$.*

Proof. Note that $I(D, \epsilon, \rho)$ is the difference in Maslov indices between $\mathbf{x}$ (in the original grid diagram) and $\tilde{\mathbf{y}} = U_1^{N_1} \cdots U_n^{N_n} \cdot (\mathbf{y}, \epsilon)$ (in the destabilized diagram), cf. Equation (24). Because $\mu(\phi)$ is additive with respect to pre- or post-composition with rectangles, we must have $\mu(\phi) = I(D, \epsilon, \rho) + C$, where C is a constant that only depends on the grid. To compute C, consider the trivial enhanced domain with $D = 0, \epsilon = (0, \dots, 0), \rho = (0, \dots, 0)$. This is associated to a class ϕ whose support is a disjoint union of n polygons, all of whom are $(k+2)$-gons with three acute angles and $k-1$ obtuse angles.

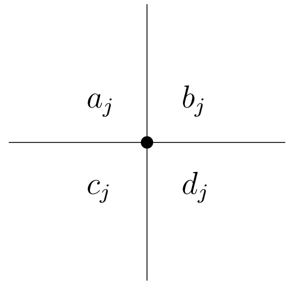

FIGURE 7. **Local multiplicities around a destabilization point.** The marked point in the middle is the destabilization point (p_j for left destabilization and q_j for right destabilization).

See Figure 8 for an example of a quadrilateral of this type. It is easy to check that $\mu(\phi) = 0$, which implies $C = 0$. $\square$

Given an enhanced domain (D, ϵ, ρ), we denote by a_j, b_j, c_j, d_j the multiplicities of D in the four squares around p_j, as in Figure 7. In particular, $b_j = t_j$ is the total multiplicity there. Note that, if $p_j \notin \mathbf{x}$, then

$$a_j + d_j = b_j + c_j + 1, \tag{26}$$

while if $p_j \in \mathbf{x}$ then

$$a_j + d_j = b_j + c_j. \tag{27}$$

Definition 3.3. *We say that the enhanced domain (D, ϵ, ρ) is* positive *if D has nonnegative multiplicities everywhere in the grid, and, furthermore, for every $j \in \{1, \dots, k\}$, we have*

$$\begin{aligned} a_j &\geq f_j, & b_j &\geq f_j, \\ c_j &\geq f_j + \epsilon_j - 1, & d_j &\geq f_j + \epsilon_j. \end{aligned} \tag{28}$$

Observe that the second of the above inequalities implies $b_j - f_j = \rho_j \geq 0$. Thus, in a positive enhanced domain, all real multiplicities ρ_j are nonnegative.

Lemma 3.4. *Suppose that (D, ϵ, ρ) is the enhanced domain associated to a homotopy class ϕ of $(k+2)$-gons as in Section 3.2, and that the homotopy class ϕ admits at least one holomorphic representative. Then (D, ϵ, ρ) is positive, in the sense of Definition 3.3.*

Proof. If a homotopy class ϕ has at least one holomorphic representative it has positive multiplicities (for suitable choices of almost-complex structure on the symmetric product, see for example Lemma 3.2 of [22]). It follows now that D has nonnegative multiplicities everywhere in the grid and that $\rho_j = b_j - f_j \geq 0$. It remains to check the three other relations.

For concreteness, let us consider the case $k = 2$, with $\epsilon_j = 0$, cf. Figure 8. The two circles encircling the destabilization point in the middle are of the type $\beta^{\{Z_1\}}$ (the right one) and $\beta^{\{Z_1, Z_2\}}$ (the left one).

If we are given the domain of a holomorphic quadrilateral (for instance, the shaded one in Figure 8), at most of the intersection points the alternating sum of nearby multiplicities is zero. The only exceptions are the four bulleted points in the figure, which correspond to the vertices of the quadrilateral, and where the alternating sum of nearby multiplicities is ± 1. (At the central intersection between an alpha and an original beta curve, there may not be a vertex and the alternating sum of the multiplicities may be 0.) If u_j, v_j, and w_j are the multiplicities in the regions indicated

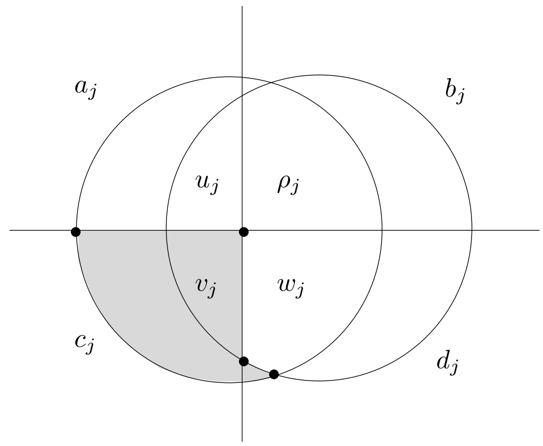

FIGURE 8. **Local multiplicities in detail.** This is a more detailed version of Figure 7, in which we show two other types of beta curves: $\beta^{\{Z_1\}}$ and $\beta^{\{Z_1,Z_2\}}$. We mark the local multiplicity in each region. The shaded region is the domain of a quadrilateral of index zero.

in Figure 8, by adding up suitable such relations between local multiplicities, we obtain

$$\begin{aligned} a_j - f_j = a_j + \rho_j - b_j \quad &= u_j \geq 0 \\ c_j - f_j + 1 = c_j + \rho_j - b_j + 1 &= v_j \geq 0 \\ d_j - f_j = d_j + \rho_j - b_j \quad &= w_j \geq 0, \end{aligned}$$

as desired. The proof in the $\epsilon_j = 1$ case, or for other values of k, is similar. □

Note that an enhanced domain $E = (D, \epsilon, \rho)$ is determined by its initial point $\mathbf{x}$ and final point $\tilde{\mathbf{y}} = U_1^{N_1} \cdots U_n^{N_n} \cdot (\mathbf{y}, \epsilon)$ up to the addition to D of linear combinations of *periodic domains* of the following form:

- A column minus the row containing the same O_i;
- A column containing one of the O_{i_j}'s used for destabilization.

When we add a column of the latter type, the total multiplicity t_j (and hence also the fake multiplicity f_j) increase by 1. The real multiplicity ρ_j does not change.

Definition 3.5. *We say that the pair* $[\mathbf{x}, \tilde{\mathbf{y}}]$ *is* positive *if there exists a positive enhanced domain with* $\mathbf{x}$ *and* $\tilde{\mathbf{y}}$ *as its initial and final points.*

3.3. **Positive domains of negative index.** Figure 9 shows some examples of positive enhanced domains of negative index, in a twice destabilized grid. We see that the index can get as negative as we want, even if we fix the number of destabilizations at two (but allow the size of the grid to change).

However, this phenomenon is impossible for one destabilization:

Proposition 3.6. *Let G be a toroidal grid diagram with only one O marked for destabilization. Then any positive enhanced domain has nonnegative index. Furthermore, if the enhanced domain is positive and has index zero, then it is of one of the types from the sequences in Figure 6.*

Proof. Let us first consider a positive enhanced domain (D, ϵ, ρ) going between the generators $\mathbf{x}$ and $\tilde{\mathbf{y}} = U_1^{N_1} \cdots U_n^{N_n} \cdot (\mathbf{y}, \epsilon)$. With the notations of Section 3.2, we have $k = 1$, $\epsilon_1 \in \{0, 1\}$ (corresponding to the type of the domain, L or R), a_1, $b_1 = t_1$, c_1, d_1 are the local multiplicities around the destabilization point, and ρ_1 and $f_1 = t_1 - \rho_1$ are the real and fake multiplicities there. Note that $t_1 \geq f_1$.

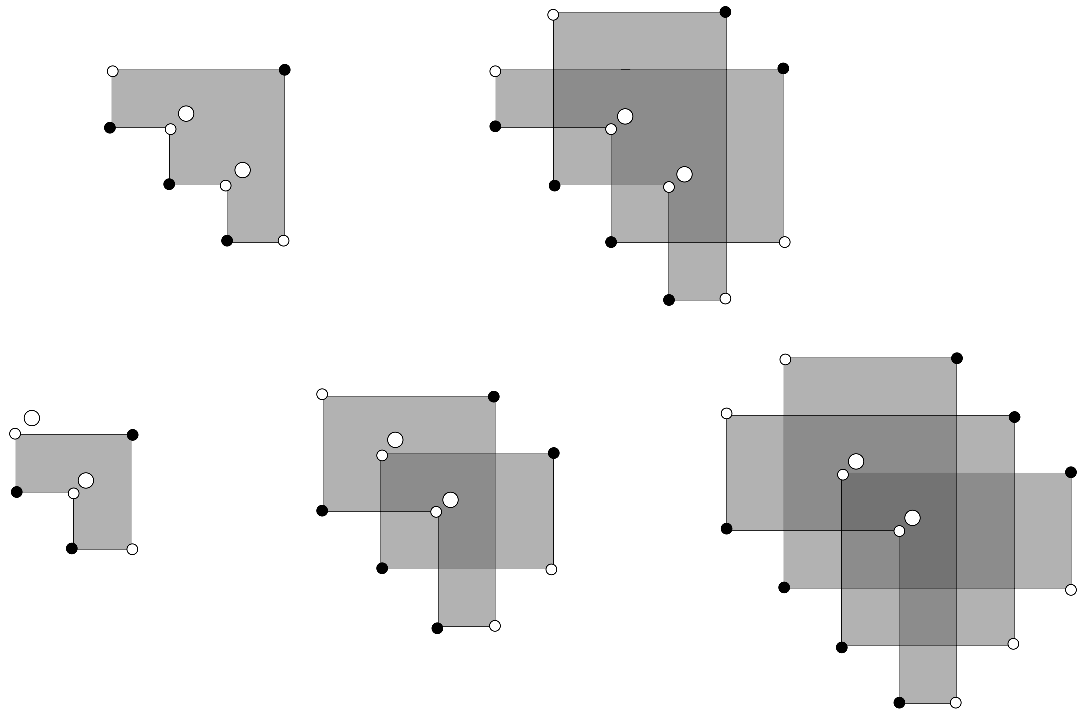

FIGURE 9. **Positive domains of negative index.** We destabilize at two O's, marked by the two larger circles in the picture. The top row shows two positive domains of type LL, the first of index -1, the second of index -2. The second row shows three positive domains of type RL, of indices $-1, -2$ and -3, respectively. Darker shading corresponds to higher local multiplicities. In each case, the real multiplicity ρ_j is zero.

Without loss of generality we can assume that every row or column contains at least one square where the multiplicity of D is zero; otherwise we could subtract that row or column and obtain another positive domain, whose index is at least as large. Indeed, if the row or column does not contain the destabilization point p_1 on its boundary, then subtracting it decreases the index by 2. If we subtract the row just to the left of p_1, or the column just below p_1, by simultaneously increasing ρ_1 by one we can preserve the positivity conditions and leave the index the same. If we subtract the row or column through the O marked for destabilization, while leaving ρ unchanged, the positivity and the index are again unaffected.

We say that a row or a column is *special* if $\mathbf{x}$ and $\mathbf{y}$ intersect it in different points. Let m be the number of special rows; it is the same as the number of special columns. Note that, as we move fro a row (or column) curve, the multiplicity of the domain D can only change by ± 1, and it can do that only if the row (or column) is special. This is because of our assumption that we have zeros in every row and column.

Let us look at the column containing the destabilized O. The domain has multiplicity d_1 in the spot right below O, and it has multiplicity zero on some other spot on that column. We can move from O to the multiplicity zero spot either by going up or down. As we go in either direction, we must encounter at least d_1 special rows. This means that the total number of special rows is at least $2d_1$. Using the fourth inequality in (28), we get

$$m \geq 2d_1 \geq 2(f_1 + \epsilon_1). \tag{29}$$

The ordinary index of the domain D is given by Equation (25), involving the sums of the average local multiplicities of D at the points of $\mathbf{x}$ and $\mathbf{y}$. One such point is the destabilization point p_1 which is part of $\mathbf{y}$. Using the relations in Equation (28), we find that the average vertex multiplicity there is

$$\frac{a_1 + b_1 + c_1 + d_1}{4} \geq f_1 + \frac{2\epsilon_1 - 1}{4}. \tag{30}$$

On the other hand, apart from the destabilization point, $\mathbf{x}$ and $\mathbf{y}$ together have either $2m - 1$ (if $p_1 \notin \mathbf{x}$) or $2m$ (if $p_1 \in \mathbf{x}$) corner vertices, where the average multiplicity has to be at least $1/4$. Together with Equations (29) and (30), this implies that

$$I(D) \geq \frac{2m-1}{4} + f_1 + \frac{2\epsilon_1 - 1}{4}. \tag{31}$$

Using the formula for the index of an enhanced domain, together with Equations (29) and (31), we obtain

$$I(D, \epsilon, \rho) = I(D) - \epsilon_1 - 2f_1 \geq \frac{m}{2} - f_1 - \frac{\epsilon_1}{2} - \frac{1}{2} \geq \frac{\epsilon_1 - 1}{2}. \tag{32}$$

Since the index is an integer, we must have $I(D, \epsilon, \rho) \geq 0$. Equality happens only when D has average vertex multiplicity $1/4$ at all its corners other than the destabilization point. An easy analysis shows that the domain must be of the required shape. $\square$

3.4. **Holomorphic triangles on grid diagrams.**

Lemma 3.7. *Fix a snail-like domain D (as in Figure 6) for destabilization at one point. Then the count of holomorphic triangles in $\mathrm{Sym}^n(\mathcal{T})$ with D as their shadow is one mod 2.*

Proof. The trivial domain D of type L corresponds to a homotopy class ϕ whose support is a disjoint union of triangles with $90°$ angles. Hence, the corresponding holomorphic count is one.

To establish the claim in general, note that the destabilization map at one point (given by counting holomorphic triangles) is a chain map (in fact, a quasi-isomorphism) from $C^-(G)$ to $EC^-(G, \mathcal{Z})$, compare (23). By Proposition 3.6, the only counts involved in this map are the ones corresponding to snail-like domains. If to each snail-like domain we assign the coefficient one when counting it in the map, the result is the chain map (23). By induction on complexity, along the lines of [14, Lemma 3.5], we do indeed need to assign one to each snail-like domain in order for the result to be a chain map. $\square$

Proposition 3.6 and Lemma 3.7 imply that one can count combinatorially (mod 2) all the index zero holomorphic triangles in a grid diagram (with one point marked for destabilization) with fixed shadow. Indeed, if the shadow is a snail-like domain, then the count is one, and otherwise it is zero.

4. Formal complex structures and surgery

Let $\vec{L} \subset S^3$ be a link with framing Λ, and let $\mathfrak{u}$ be a Spin^c structure on the surgered manifold $S^3_\Lambda(L)$. Our goal in this section is to explain a combinatorial procedure for calculating the ranks of the groups $\mathbf{HF}^-(S^3_\Lambda(L), \mathfrak{u})$. The procedure will be based on Theorem 2.5. The algorithm is made more complicated because Proposition 3.6 and therefore Lemma 3.7 are false if there is more than one destabilization point; we therefore have to make an appropriate choice of domains to count, a choice we call a "formal complex structure".

4.1. **The complex of positive pairs.** Let G be a grid diagram (of size n) marked for destabilization at a collection $\mathcal{Z}$ of some O's, with $|\mathcal{Z}| = k < n$, as in Section 3.2. In that section we defined the (quasi-isomorphic) complexes $C^-(G)$ and $EC^-(G, \mathcal{Z})$. Let us consider the Hom complex

$$\mathrm{Hom}_{\mathcal{R}}(C^-(G), EC^-(G, \mathcal{Z})),$$

where $\mathcal{R} = \mathbb{F}[[U_1, \dots, U_n]]$. Since $C^-(G)$ is a free $\mathcal{R}$-module, we can naturally identify it with its dual using the basis given by $\mathbf{S}(G)$. Thus, if we view the Hom complex as an $\mathbb{F}$-vector space, its generators (in the sense of direct products) are pairs $[\mathbf{x}, \tilde{\mathbf{y}}]$, where $\tilde{\mathbf{y}}$ is an enhanced generator possibly multiplied by some powers of U, i.e., $\tilde{\mathbf{y}} = U_1^{N_1} \cdots U_n^{N_n} \cdot (\mathbf{y}, \epsilon)$.

The homological degree of a generator in the Hom complex is $M(\tilde{\mathbf{y}}) - M(\mathbf{x})$. However, we would like to think of the generators as being enhanced domains (up to the addition of periodic domains), so in order to be consistent with the formula for the index of domains we set

$$I([\mathbf{x}, \tilde{\mathbf{y}}]) = M(\mathbf{x}) - M(\tilde{\mathbf{y}})$$

and view the Hom complex as a cochain complex, with a differential d that increases the grading. It has the structure of an $\mathcal{R}$-module, where multiplication by a variable U_i increases the grading by two: $U_i[\mathbf{x}, \tilde{\mathbf{y}}] = [\mathbf{x}, U_i\tilde{\mathbf{y}}]$. Note that the Hom complex is bounded from below with respect to the Maslov grading.

There is a differential on the complex given by

$$d[\mathbf{x}, \tilde{\mathbf{y}}] = [\partial^* \mathbf{x}, \tilde{\mathbf{y}}] + [\mathbf{x}, \partial \tilde{\mathbf{y}}].$$

Thus, taking the differential of a domain consists in summing over the ways of pre- and post-composing the domain with a rectangle.

If a pair $[\mathbf{x}, \tilde{\mathbf{y}}]$ is positive (as in Definition 3.5), then by definition it represents a positive domain; adding a rectangle to it keeps it positive. Indeed, note that if the rectangle crosses an O used for destabilization, then the real and total multiplicities increase by 1, but the fake multiplicity stays the same, so the inequalities (28) are still satisfied.

Therefore, the positive pairs $[\mathbf{x}, \tilde{\mathbf{y}}]$ generate a subcomplex $CP^*(G, \mathcal{Z})$ of the Hom complex. For the moment, let us ignore its structure as an $\mathcal{R}$-module, and simply consider it as a cochain complex over $\mathbb{F}$. We denote its cohomology by $HP^*(G, \mathcal{Z})$.

We make the following:

Conjecture 4.1. *Let G be a toroidal grid diagram of size n with a collection $\mathcal{Z}$ of O's marked for destabilization, such that $|\mathcal{Z}| < n$. Then $HP^d(G, \mathcal{Z}) = 0$ for $d < 0$.*

Proposition 3.6 implies Conjecture 4.1 in the case when only one O is marked for destabilization. Indeed, in that case we have $CP^d(G, \mathcal{Z}) = 0$ for $d < 0$, so the homology is also zero.

In the case of several destabilization points, we can prove only a weaker form of the conjecture, namely Theorem 4.3 below. However, this will suffice for our application.

Definition 4.2. *Let G be a toroidal grid diagram of size $n > 1$, with a collection $\mathcal{Z}$ of some O's marked for destabilization. If none of the O's marked for destabilization sit in adjacent rows or adjacent columns, we say that the pair $(G, \mathcal{Z})$ is* sparse. *(Note that if $(G, \mathcal{Z})$ is sparse, we must have $|\mathcal{Z}| \leq (n+1)/2 < n$.)*

Recall that in the Introduction we gave a similar definition, which applies to grid diagrams G (with free markings) representing links in S^3. Precisely, we said that G is *sparse* if none of the linked markings sit in adjacent rows or in adjacent columns. Observe that, if G is sparse, then the pair $(G, \mathcal{Z})$ is sparse for any collection $\mathcal{Z}$ of linked markings.

Theorem 4.3. *If $(G, \mathcal{Z})$ is a sparse toroidal grid diagram with k O's marked for destabilization, then $HP^d(G, \mathcal{Z}) = 0$ for $d < \min\{0, 2-k\}$.*

Once we show this, it will also follow that, for $(G, \mathcal{Z})$ sparse, the homology of $CP^*(G, \mathcal{Z}) \otimes M$ is zero in degrees $< \min\{0, 2-k\}$, where M is an $\mathcal{R}$-module (a quotient of $\mathcal{R}$) obtained by setting some of the U variables equal to each other.

The proof of Theorem 4.3 will be given in Section 5.

4.2. **An extended complex of positive pairs.** Let us now return to the set-up of Section 2, where $\vec{L}$ is an oriented link with a grid presentation G of grid number n, and with $q \geq 1$ free markings.

When $\mathcal{Z}$ is a consistent set of linked markings (X's or O's) on G, we set

$$J_\infty(\mathcal{Z}) = \{\mathbf{s} = (s_1, \dots, s_\ell) \in J(\mathcal{Z}) \mid s_i = \pm\infty \text{ for all } i\}.$$

Let $\mathcal{Z}_0$ and $\mathcal{Z}$ be two disjoint sets of linked markings on G such that $\mathcal{Z}_0 \cup \mathcal{Z}$ is consistent. For $\mathbf{s} \in J_\infty(\mathcal{Z}_0 \cup \mathcal{Z})$, we can define a cochain complex

$$CP^*(G; \mathcal{Z}_0, \mathcal{Z}, \mathbf{s}),$$

which is the subcomplex of

$$\operatorname{Hom}_{\mathcal{R}}\big(\mathfrak{A}^-(\mathbb{T}_\alpha, \mathbb{T}_\beta^{\mathcal{Z}_0}, \mathbf{s}), \mathfrak{A}^-(\mathbb{T}_\alpha, \mathbb{T}_\beta^{\mathcal{Z}_0 \cup \mathcal{Z}}, \mathbf{s})\big) \tag{33}$$

spanned by positive pairs. Here positivity of pairs has the same meaning as before: it is defined in terms of enhanced domains, by looking at the grid diagram $G^{\mathcal{Z}_0}$ destabilized at the points of $\mathcal{Z}_0$.

Lemma 4.4. *If $\mathcal{Z}_0 \amalg \mathcal{Z}$ is a consistent set of linked markings on a grid G and $\mathbf{s}, \mathbf{s}' \in J_\infty(\mathcal{Z}_0 \cup \mathcal{Z})$, then the complexes $CP^*(G; \mathcal{Z}_0, \mathcal{Z}, \mathbf{s})$ and $CP^*(G; \mathcal{Z}_0, \mathcal{Z}, \mathbf{s}')$ are canonically isomorphic.*

Proof. It suffices to consider the case when $\mathbf{s}$ and $\mathbf{s}'$ differ in only one place, say $s_i \neq s_i'$ for a component $L_i \not\subseteq L(\mathcal{Z}_0 \cup \mathcal{Z})$, where $L(\mathcal{Z}_0 \cup \mathcal{Z})$ is as in Section 2.6. Suppose $s_i = -\infty$ while $s_i' = +\infty$. Then the desired isomorphism is

$$CP^*(G; \mathcal{Z}_0, \mathcal{Z}, \mathbf{s}) \longrightarrow CP^*(G; \mathcal{Z}_0, \mathcal{Z}, \mathbf{s}'), \quad [\mathbf{x}, \tilde{\mathbf{y}}] \to U_i^{A_i(\mathbf{x}) - A_i(\mathbf{y})}[\mathbf{x}, \tilde{\mathbf{y}}], \tag{34}$$

where $\tilde{\mathbf{y}} = U_1^{N_1} \cdots U_\ell^{N_\ell}(\mathbf{y}, \epsilon)$ and A_i is the component of the Alexander grading corresponding to L_i. To verify that this is a well-defined map, we proceed as follows. If D is a positive domain representing the pair $[\mathbf{x}, \tilde{\mathbf{y}}]$, note that

$$A_i(\mathbf{x}) - A_i(\mathbf{y}) = \sum_{j \in \mathbb{X}_i} X_i(D) - \sum_{j \in \mathbb{O}_i} O_i(D)$$

and $N_i = \sum_{j \in \mathbb{O}_i} O_i(D)$, so

$$A_i(\mathbf{x}) - A_i(\mathbf{y}) + N_i = \sum_{j \in \mathbb{X}_i} X_i(D) \geq 0.$$

This implies that $U_i^{A_i(\mathbf{x}) - A_i(\mathbf{y})}[\mathbf{x}, \tilde{\mathbf{y}}]$ is an element of $CP^*(G; \mathcal{Z}_0, \mathcal{Z}, \mathbf{s}')$, with the same domain D as a positive representative. One can then easily check that the map from Equation (34) is a chain map.

The inverse of (34) is also a positivity-preserving chain map, this time given by multiplication with $U_i^{A_i(\mathbf{y}) - A_i(\mathbf{x})}$. Indeed, a similar argument applies: a positive domain D representing a pair $[\mathbf{x}, \tilde{\mathbf{y}}]$ in $CP^*(G; \mathcal{Z}_0, \mathcal{Z}, \mathbf{s}')$ has $N_i = \sum_{j \in \mathbb{X}_i} X_i(D)$, and we get $A_i(\mathbf{y}) - A_i(\mathbf{x}) + N_i \geq 0$. ☐

In view of Lemma 4.4, we can drop $\mathbf{s}$ from the notation and refer to $CP^*(G; \mathcal{Z}_0, \mathcal{Z}, \mathbf{s})$ simply as $CP^*(G; \mathcal{Z}_0, \mathcal{Z})$.

Let $G^{\mathcal{Z}_0, \mathcal{Z}}$ be the grid diagram $G^{\mathcal{Z}_0}$ with all X markings on components $L_i \not\subseteq L(\mathcal{Z}_0 \cup \mathcal{Z})$ deleted and the remaining X markings relabeled as O. Further, we mark for destabilization the markings in $\mathcal{Z}$. Then $(G^{\mathcal{Z}_0, \mathcal{Z}}, \mathcal{Z})$ is a grid diagram with only O's, some of them marked for destabilization, as in Sections 3.2 and 4.1. As such, it has a complex of positive pairs $CP^*(G^{\mathcal{Z}_0, \mathcal{Z}}, \mathcal{Z})$, cf. Section 4.1.

In light of the isomorphisms (11), we see that

$$CP^*(G;\mathcal{Z}_0,\mathcal{Z}) \cong CP^*(G^{\mathcal{Z}_0,\mathcal{Z}},\mathcal{Z}) \otimes M, \tag{35}$$

where M is an $\mathcal{R}$-module obtained by setting some U variables equal to each other.

Let $\mathcal{Z}_0, \mathcal{Z}, \mathcal{Z}'$ be disjoint sets of linked markings on G, such that $\mathcal{Z}_0 \cup \mathcal{Z} \cup \mathcal{Z}'$ is consistent. There are natural composition maps

$$\circ : CP^i(G;\mathcal{Z}_0 \cup \mathcal{Z},\mathcal{Z}') \otimes CP^j(G;\mathcal{Z}_0,\mathcal{Z}) \to CP^{i+j}(G;\mathcal{Z}_0,\mathcal{Z}\cup\mathcal{Z}'), \tag{36}$$

obtained from the respective Hom complexes by restriction.

We define the *extended complex of positive pairs* associated to G to be

$$CE^*(G) = \bigoplus_{\mathcal{Z}_0,\mathcal{Z}} CP^*(G;\mathcal{Z}_0,\mathcal{Z}),$$

where the direct sum is over all collections $\mathcal{Z}_0, \mathcal{Z}$ such that $\mathcal{Z}_0 \cup \mathcal{Z}$ is consistent.

This breaks into a direct sum

$$CE^*(G) = \bigoplus_{k=0}^{n-q} CE^*(G;k),$$

according to the cardinality k of $\mathcal{Z}$, i.e., the number of points marked for destabilization. Putting together the maps (36), we obtain global composition maps:

$$\circ : CE^i(G;k) \otimes CE^j(G;l) \to CE^{i+j}(G;k+l), \tag{37}$$

where the compositions are set to be zero when not a priori well-defined on the respective summands. These composition maps satisfy a Leibniz rule for the differential.

The complex $CE^*(G)$ was mentioned in the Introduction. There we stated Conjecture 1.1, which says that for any toroidal grid diagram G, we have

$$HE^d(G) = 0 \text{ when } d < 0.$$

Observe that Conjecture 1.1 would be a direct consequence of Conjecture 4.1, because of Equation (35).

We prove a weaker version of Conjecture 1.1, which applies only to sparse grid diagrams (as defined in the Introduction).

Theorem 4.5. *Let G be a sparse toroidal grid diagram representing a link L. Then $HE^d(G;k) = 0$ whenever $d < \min\{0, 2-k\}$.*

Proof. This follows from Theorem 4.3, using Equation (35). The key observation is that all destabilizations of a sparse diagram at linked markings are also sparse. □

4.3. **Formal complex structures.** Let G be a grid presentation for the link L, such that G has $q \geq 1$ free markings. Our goal is to find an algorithm for computing $\mathbf{HF}^-_*(S^3_\Lambda(L),\mathfrak{u})$, where Λ is a framing of L and $\mathfrak{u}$ a Spin^c structure on $S^3_\Lambda(L)$. We will first describe how to do so assuming that Conjecture 1.1 is true, and using Theorem 2.5.

By Theorem 2.5, we need to compute the homology of the complex $\mathcal{C}^-(G,\Lambda,\mathfrak{u}) \subseteq \mathcal{C}^-(G,\Lambda)$, with its differential $\mathcal{D}^-$. In the definition of $\mathcal{D}^-$ we use the maps $\Phi^{\vec{M}}_{\mathbf{s}}$, which in turn are based on destabilization maps $\hat{D}^{\vec{M}}_{\mathbf{s}}$ of the kind constructed in Section 2.7. In turn, the maps $\hat{D}^{\vec{M}}_{\mathbf{s}}$, obtained by compression, are sums of compositions of maps of the type $D^{\mathcal{Z}}_{\mathbf{s}}$ (for unordered sets of markings $\mathcal{Z}$), as in Section 2.4.

Consider the maps

$$D^{\mathcal{Z}}_{\mathbf{s}} : \mathfrak{A}^-(\mathbb{T}_\alpha, \mathbb{T}^{\mathcal{Z}_0}_\beta, \mathbf{s}) \to \mathfrak{A}^-(\mathbb{T}_\alpha, \mathbb{T}^{\mathcal{Z}_0\cup\mathcal{Z}}_\beta, \mathbf{s}), \tag{38}$$

for $\mathbf{s} \in J(\mathcal{Z}_0 \cup \mathcal{Z})$, compare Remark 2.3. Each such map is defined by counting holomorphic $(k+2)$-gons of index $1-k$ in $\mathrm{Sym}^n(\mathcal{T})$, where k is the cardinality of $\mathcal{Z}$. The holomorphic polygon counts that appear are the same regardless of the value $\mathbf{s} \in J(\mathcal{Z}_0 \cup \mathcal{Z})$. Hence, if we fix $\mathcal{Z}_0$ and $\mathcal{Z}$, the map $D^{\mathcal{Z}}_{\mathbf{s}}$ for one value of $\mathbf{s}$ determines those for all other $\mathbf{s}$.

Remark 4.6. One instance of this principle can be seen at the level of the maps $D^{\vec{M}}_{\mathbf{s}}$ defined in Equation (15). Fixing $\vec{M}$, the maps $D^{\vec{M}}_{\mathbf{s}}$ are determined by the map for one value of $\mathbf{s} \in J(\vec{M})$, using Equation (16). Indeed, in that situation the respective inclusion maps $\mathcal{I}^{\vec{M}}_{\mathbf{s}}$ are invertible, essentially because they satisfy Equation (16). Hence, taking $\vec{M}_1 = \vec{M}$ and $\vec{M}_2 = \vec{L} - M$, we find that the map $D^{\vec{M}}_{\mathbf{s}}$ is determined by $D^{\vec{M}}_{p^{\vec{L}-M}(\mathbf{s})}$.

Pick some $\mathbf{s} \in J_\infty(\mathcal{Z}_0 \cup \mathcal{Z}) \subset J(\mathcal{Z}_0 \cup \mathcal{Z})$. We will focus on the map (38) for that value $\mathbf{s}$. We seek to understand the map $D^{\mathcal{Z}}_{\mathbf{s}}$ combinatorially.

In the case $k=0$, we know that holomorphic bigons are the same as empty rectangles on $\mathcal{T}$, cf. [13]. For $k=1$, one can still count holomorphic triangles explicitly, cf. Section 3.4.

Unfortunately, for $k \geq 2$, the count of holomorphic $(k+2)$-gons seems to depend on the almost complex structure on $\mathrm{Sym}^n(\mathcal{T})$. The best we can hope for is not to calculate the maps $D^{\mathcal{Z}}$ explicitly, but to calculate them up to chain homotopy. In turn, this will give an algorithm for computing the chain complex $\mathcal{C}^-(G, \Lambda, \mathfrak{u})$ up to chain homotopy equivalence, and this is enough for knowing its homology.

Recall that a complex structure j on the torus $\mathcal{T}$ gives rise to a complex structure $\mathrm{Sym}^n(j)$ on the symmetric product $\mathrm{Sym}^n(\mathcal{T})$. In [22], in order to define Floer homology the authors used a certain class of perturbations of $\mathrm{Sym}^n(j)$, which are (time dependent) almost complex structures on $\mathrm{Sym}^n(\mathcal{T})$. For each almost complex structure J in this class, one can count J-holomorphic polygons for various destabilization maps. In particular, for any

$$\mathbf{x} \in \mathbb{T}_\alpha \cap \mathbb{T}^{\mathcal{Z}_0}_\beta, \quad \mathbf{y} \in \mathbb{T}_\alpha \cap \mathbb{T}^{\mathcal{Z}_0 \cup \mathcal{Z}}_\beta, \ \tilde{\mathbf{y}} = U_1^{i_1} \cdots U_{\ell+q}^{i_{\ell+q}}(\mathbf{y}, \epsilon)$$

there is a number

$$n^{\mathcal{Z}_0, \mathcal{Z}}_J(\mathbf{x}, \tilde{\mathbf{y}}) \in \mathbb{F}$$

such that the destabilization map (38) is given by

$$D^{\mathcal{Z}}_{\mathbf{s}} \mathbf{x} = \sum_{\mathbf{y}} n^{\mathcal{Z}_0, \mathcal{Z}}_J(\mathbf{x}, \tilde{\mathbf{y}}) \cdot \tilde{\mathbf{y}}.$$

In other words, $n^{\mathcal{Z}_0, \mathcal{Z}}_J(\mathbf{x}, \mathbf{y})$ is the count of J-holomorphic $(k+2)$-gons between $\mathbf{x}$ and $\tilde{\mathbf{y}}$, in all possible homotopy classes ϕ with $\mu(\mathbf{x}, \mathbf{y}) = \mu(\phi) = 1-k$, and coming from all possible orderings of the elements of $\mathcal{Z}$. (Recall that $D^{\mathcal{Z}}$ is a sum of maps of the form $D^{(Z_1, \dots, Z_k)}$, where $(Z_1, \dots, Z_k)$ is an ordering of $\mathcal{Z}$.)

Observe that, in order for $n^{\mathcal{Z}_0, \mathcal{Z}}_J(\mathbf{x}, \tilde{\mathbf{y}})$ to be nonzero, the pair $[\mathbf{x}, \tilde{\mathbf{y}}]$ has to be positive. Hence, the set of values $n^{\mathcal{Z}_0, \mathcal{Z}}_J(\mathbf{x}, \tilde{\mathbf{y}})$ produces well-defined elements in the extended complex of positive pairs on G:

$$c_k(J) = \sum n^{\mathcal{Z}_0, \mathcal{Z}}_J(\mathbf{x}, \tilde{\mathbf{y}}) \cdot [\mathbf{x}, \tilde{\mathbf{y}}] \in CP^{1-k}(G; \mathcal{Z}_0, \mathcal{Z}) \subseteq CE^{1-k}(G; k), \quad k \geq 1.$$

Lemma 2.2 implies that the elements $c_k(J)$ satisfy the following compatibility conditions, with respect to the composition product (37):

$$dc_k(J) = \sum_{i=1}^{k-1} c_i(J) \circ c_{k-i}(J).$$

In particular, $dc_1(J) = 0$. Note that $c_1(J)$ is given by the count of snail-like domains, and therefore is independent of J. We denote it by

$$c_1^{\mathrm{sn}} \in CE^0(G; 1).$$

Definition 4.7. *A* formal complex structure $\mathfrak{c}$ *on the grid diagram G (of grid number n, and with $q \geq 1$ free markings) consists of a family of elements*

$$c_k \in CE^{1-k}(G; k), \quad k = 1, \dots, n-q,$$

satisfying $c_1 = c_1^{\mathrm{sn}}$ and the compatibility conditions:

$$dc_k = \sum_{i=1}^{k-1} c_i \circ c_{k-i}. \tag{39}$$

In particular, an (admissible) almost complex structure J on $\mathrm{Sym}^n(\mathcal{T})$ induces a formal complex structure $\mathfrak{c}(J)$ on G.

Remark 4.8. If we let $\mathfrak{c} = (c_1, c_2, \dots) \in CE^*(G)$, the relation (39) is summarized by the equation

$$d\mathfrak{c} = \mathfrak{c} \circ \mathfrak{c}. \tag{40}$$

Definition 4.9. *Two formal complex structures $\mathfrak{c} = (c_1, c_2, \dots), \mathfrak{c}' = (c_1', c_2', \dots)$ on a grid diagram G (of grid number n, with $q \geq 1$ free markings) are called* homotopic *if there exists a sequence of elements*

$$h_k \in CE^{-k}(G; k), \quad k = 1, \dots, n-q$$

satisfying $h_1 = 0$ and

$$c_k - c_k' = dh_k + \sum_{i=1}^{k-1} \big(c_i' \circ h_{k-i} + h_i \circ c_{k-i} \big). \tag{41}$$

Observe that, if J and J' are (admissible) almost complex structures on $\mathrm{Sym}^n(\mathcal{T})$, one can interpolate between them by a family of almost complex structures. The resulting counts of holomorphic $(2+k)$-gons of index $-k$ induce a homotopy between $\mathfrak{c}(J)$ and $\mathfrak{c}(J')$. There is therefore a canonical homotopy class of formal complex structures that come from actual almost complex structures.

Lemma 4.10. *Assume $HE^{1-k}(G; k) = 0$ for any $k = 2, \dots, n-q$. Then any two formal complex structures on G are homotopic.*

Proof. Let $\mathfrak{c} = (c_1, c_2, \dots), \mathfrak{c}' = (c_1', c_2', \dots)$ be two formal complex structures on G. We prove the existence of the elements h_k by induction on k. When $k = 1$, we have $c_1 = c_1' = c_1^{\mathrm{sn}}$ so we can take $h_1 = 0$.

Assume we have constructed h_i for $i < k$ satisfying (41), and we need h_k. Since by hypothesis the cohomology group $CE(G; k)$ is zero in degree $1 - k$, it suffices to show that

$$c_k - c_k' - \sum_{i=1}^{k-1} \big(c_i' \circ h_{k-i} + h_i \circ c_{k-i} \big) \tag{42}$$

is a cocycle. Indeed, we have

$$\begin{aligned}
&d\Big(c_k - c_k' - \sum_{i=1}^{k-1} \big(c_i' \circ h_{k-i} + h_i \circ c_{k-i} \big) \Big) \\
&\quad = \sum_{i=1}^{k-1} c_i \circ c_{k-i} - \sum_{i=1}^{k-1} c_i' \circ c_{k-i}' - \sum_{i=1}^{k-1} \big(dc_i' \circ h_{k-i} + c_i' \circ dh_{k-i} + dh_i \circ c_{k-i} + h_i \circ dc_{k-i} \big) \\
&\quad = \sum_{i=1}^{k-1} (c_i - c_i' - dh_i) \circ c_{k-i} + \sum_{i=1}^{k-1} c_i' \circ (c_{k-i} - c_{k-i}' - dh_{k-i}) - \sum_{i=1}^{k-1} dc_i' \circ h_{k-i} - \sum_{i=1}^{k-1} h_i \circ dc_{k-i} \\
&\quad = \sum (c_\alpha' h_\beta c_\gamma + h_\alpha c_\beta c_\gamma) + \sum (c_\alpha' h_\beta c_\gamma + c_\alpha' c_\beta' h_\gamma) - \sum c_\alpha' c_\beta' h_\gamma - \sum h_\alpha c_\beta c_\gamma \\
&\quad = 0.
\end{aligned}$$

In the second-to-last line the summations are over $\alpha, \beta, \gamma \geq 1$ with $\alpha+\beta+\gamma = k$, and we suppressed the composition symbols for simplicity. $\square$

4.4. **Combinatorial descriptions.** Consider a formal complex structure $\mathfrak{c}$ on a grid G (of grid number n, with $q \geq 1$ free markings), a framing Λ for L, and an equivalence class $\mathfrak{u} \in \big(\mathbb{H}(L)/H(L,\Lambda)\big) \cong \mathrm{Spin}^c(S^3_\Lambda(L))$. We seek to define a complex $\mathcal{C}^-(G,\Lambda,\mathfrak{u},\mathfrak{c})$ analogous to the complex $\mathcal{C}^-(G,\Lambda,\mathfrak{u})$ from Section 2.8, but defined using the elements c_k instead of the holomorphic polygon counts. (In particular, if $\mathfrak{c} = \mathfrak{c}(J)$ for an actual almost complex structure J, we want to recover the complex $\mathcal{C}^-(G,\Lambda,\mathfrak{u})$ from Section 2.8.)

Let us explain the construction of $\mathcal{C}^-(G,\Lambda,\mathfrak{u},\mathfrak{c})$. Recall that in Section 2.8 the complex $\mathcal{C}^-(G,\Lambda,\mathfrak{u})$ was built by combining hypercubes of the form $\mathcal{H}^{\mathcal{Z}}_{\mathbf{s}}$, for various consistent sets of linked markings $\mathcal{Z}$ and values $\mathbf{s} \in J(\mathcal{Z})$. We can define analogous hypercubes $\mathcal{H}^{\mathcal{Z}}_{\mathbf{s}}(\mathfrak{c})$, by counting $(k+2)$-gons according to the coefficients of enhanced domains that appear in $\mathfrak{c}_k$.

Taking into account the naturality properties of compression discussed at the end of Section 2.1, the proof of the following lemma is straightforward:

Lemma 4.11. *A homotopy between formal complex structures $\mathfrak{c}, \mathfrak{c}'$ on G induces a chain homotopy equivalence between the complexes $\mathcal{C}^-(G,\Lambda,\mathfrak{u},\mathfrak{c})$ and $\mathcal{C}^-(G,\Lambda,\mathfrak{u},\mathfrak{c}')$.*

With this in mind, we are ready to prove the two theorems advertised in the Introduction.

Proof of Theorem 1.2. The algorithm to compute $\mathbf{HF}^-$ of an integral surgery on a link $\vec{L}$ goes as follows. First, choose a sparse grid diagram G for $\vec{L}$ (for example, by taking the sparse double of an ordinary grid diagram, as in Figure 1). Then, choose any formal complex structure on G, construct the complex $\mathcal{C}^-(G,\Lambda,\mathfrak{u},\mathfrak{c})$, and take its homology.

Let us explain why this algorithm is finite and gives the desired answer. Observe that $CE^*(G)$ is finite in each degree, and the number k of destabilization points is bounded above by $n-q$, so the direct sum $\oplus_{k\geq 1} CE^{1-k}(G;k)$ is a finite set. Further, we know that a formal complex structure exists, because it could be induced by some almost complex structure J. Thus, we can find a formal complex structure $\mathfrak{c}$ on G by a brute force approach: go over all the (necessarily finite) sequences $\mathfrak{c} = (c_1 = c_1^{\mathrm{sn}}, c_2, c_3, \dots) \in \oplus_{k\geq 1} CE^{1-k}(G;k)$, and pick the first one that satisfies Equation (40). Then, by Theorem 4.5 and Lemma 4.10 we know that all possible $\mathfrak{c}$'s are homotopic. Lemma 4.11, together with Theorem 2.5, tells us that the homology of $\mathcal{C}^-(G,\Lambda,\mathfrak{u},\mathfrak{c})$ is indeed the right answer (after dividing out the factor corresponding to the homology of a torus).

(We could alternately take a somewhat more efficient, step-by-step approach to finding $\mathfrak{c}$: start with $c_1 = c_1^{\mathrm{sn}}$ and inductively find each c_k for $k \geq 2$. Since Formula (42) represents a cycle, the obstruction to extending a partial formal complex structure to the next step vanishes.)

Note that although this description is combinatorial in nature, the complex $\mathcal{C}^-(G,\Lambda,\mathfrak{u},\mathfrak{c})$ is still infinite dimensional, being an infinite direct product of modules over a ring of power series. However, we can replace it by a quasi-isomorphic, finite dimensional complex over $\mathbb{F} = \mathbb{Z}/2\mathbb{Z}$ using the vertical and horizontal truncation procedures from [12, Section 6]. Taking the homology of the truncated complex is clearly an algorithmic task.

One can calculate the other versions of Heegaard Floer homology ($\mathbf{HF}^\infty, HF^+$) in a similar way, using Theorem 2.7. $\square$

Proof of Theorem 1.3. One can calculate the maps induced by two-handle additions using Theorems 2.6 and 2.7. Furthermore, we can calculate the mixed invariants of closed four-manifolds using Proposition 2.10. In all cases, one proceeds by choosing an arbitrary formal complex structure $\mathfrak{c}$ on the grid diagram G, and computing the respective groups or maps using polygon counts prescribed by $\mathfrak{c}$. $\square$

We also have the following:

Theorem 4.12. *Fix a sparse grid diagram G for an oriented link $\vec{L}' \cup \vec{L}$ in S^3. Fix also framings Λ for L and Λ' for L'. Suppose that L has ℓ components $L_1, \dots, L_\ell$. Let $Y(0, \dots, 0) = S^3_{\Lambda'}(L')$, and, for any $\varepsilon \in \mathbb{E}_\ell$, let $Y(\varepsilon)$ be obtained from $Y(0, \dots, 0)$ by surgery on the components $L_i \subseteq L$ with $\varepsilon_i = 1$. Then, all the pages of the link surgeries spectral sequence from Theorem 2.11 (with $E^1 = \oplus_{\varepsilon \in \mathbb{E}_\ell} \mathbf{CF}^-(Y(\varepsilon))$ and coefficients in $\mathbb{F} = \mathbb{Z}/2\mathbb{Z}$) are algorithmically computable.*

Proof. Use the equivalent description of the spectral sequence given in Theorem 2.13. Choose a formal complex structure $\mathfrak{c}$ on the grid diagram G, and construct a complex $\mathcal{C}^-(G, \Lambda' \cup \Lambda, \mathfrak{c} /\!\!/ L)$ analogous to $\mathcal{C}^-(G, \Lambda' \cup \Lambda /\!\!/ L)$, but using the polygon counts given by $\mathfrak{c}$. Then compute the spectral sequence associated to the depth filtration on $\mathcal{C}^-(G, \Lambda' \cup \Lambda, \mathfrak{c} /\!\!/ L)$. □

Remark 4.13. Suppose a link L has grid number m, that is, m is the lowest number such that G admits a grid presentation of that size. Our algorithms above are based on a sparse grid diagram for L, and such a diagram must have grid number at least $2m$. If Conjecture 1.1 were true, we would obtain more efficient algorithms, because we could start with a diagram of grid number only $m+1$ (by adding only one free marking to the minimal grid).

Remark 4.14. Our present techniques do not give a combinatorial procedure for finding the map $F^-_{W,\mathbf{t}}$ associated to an arbitrary cobordism map (in a given degree) or even its rank. However, suppose W is a cobordism between connected three-manifolds Y_1 and Y_2 such that the induced maps $H_1(Y_1;\mathbb{Z})/\text{Tors} \to H_1(W;\mathbb{Z})/\text{Tors}$ and $H_1(Y_2;\mathbb{Z})/\text{Tors} \to H_1(W;\mathbb{Z})/\text{Tors}$ are surjective. Then the ranks of $F^-_{W,\mathbf{t}}$ in fixed degrees can be computed using the same arguments as in [8, Section 4]. Indeed, they are determined by the ranks of the map induced by the two-handle additions which are part of the cobordism W.

5. Sparse grid diagrams

This section is devoted to the proof of Theorem 4.3. Let $(G, \mathcal{Z})$ be a sparse toroidal grid diagram with some O's marked for destabilization, as in Section 3.2. We define a filtration $\mathcal{F}$ on $CP^*(G, \mathcal{Z})$ as follows. Let us mark one X in each square of the grid with the property that neither its row nor its column contains an O marked for destabilization. (Note that these X's have nothing to do with the original set of X's from the link.) See Figure 12, where the squares marked by an X are shown shaded.

Given a pair $[\mathbf{x}, \tilde{\mathbf{y}}]$, let (D, ϵ, ρ) be an enhanced domain from $\mathbf{x}$ to $\tilde{\mathbf{y}}$. Let $X(D)$ be the number of X's inside D, counted with multiplicity. Define

$$\mathcal{F}([\mathbf{x}, \tilde{\mathbf{y}}]) = -X(D) - \sum_{j=1}^{k} \rho_j. \tag{43}$$

It is easy to see that $X(D)$ does not change under addition of periodic domains. Since the same is true for the real multiplicities ρ_j, the value $\mathcal{F}([\mathbf{x}, \tilde{\mathbf{y}}])$ is well-defined. Furthermore, pre- or post-composing with a rectangle can only decrease $\mathcal{F}$, so $\mathcal{F}$ is indeed a filtration on $CP^*(G, \mathcal{Z})$.

To show that $HP^d(G, \mathcal{Z}) = 0$ (for $d > 0$) it suffices to check that the homology of the associated graded groups to $\mathcal{F}$ are zero. In the associated graded complex $\mathrm{gr}_{\mathcal{F}}\, CP^*(G, \mathcal{Z})$, the differential only involves composing with rectangles r such that r is supported in a row or column going through some $O_{i_j} \in \mathcal{Z}$ marked for destabilization, but r does not contain O_{i_j}. We cannot post-compose with such a rectangle, because it would move the destabilization corners in $\mathbf{y}$, and that is not allowed. Thus, the differential of $\mathrm{gr}_{\mathcal{F}}\, CP^*(G, \mathcal{Z})$ only involves pre-composing with rectangles as above.

For each positive pair $\mathbf{p} = [\mathbf{x}, \tilde{\mathbf{y}}]$, we let $C\mathcal{F}^*(G, \mathcal{Z}, \mathbf{p})$ be the subcomplex of $\mathrm{gr}_{\mathcal{F}}\, CP^*(G, \mathcal{Z})$ generated by $\mathbf{p}$ and those pairs related to $\mathbf{p}$ by a sequence of nonzero differentials in $\mathrm{gr}_{\mathcal{F}}\, CP^*(G, \mathcal{Z})$. More precisely, for each complex over $\mathbb{F}$ freely generated by a set S, we can form an associated graph whose set of vertices is S and with an edge from $\mathbf{x}$ to $\mathbf{y}$ ($\mathbf{x}, \mathbf{y} \in S$) whenever the coefficient of $\mathbf{y}$ in

$d\mathbf{x}$ is one. Then the graph of $C\mathcal{F}^*(G, \mathcal{Z}, \mathbf{p})$ is the connected component containing $\mathbf{p}$ of the graph of $\mathrm{gr}_{\mathcal{F}}\, CP^*(G, \mathcal{Z})$ (with respect to the standard basis).

Definition 5.1. *Let $(G, \mathcal{Z})$ be a toroidal grid diagram with $\mathcal{Z} = \{O_{i_j} | j = 1, \dots, k\}$ marked for destabilization. The four corners of the square containing O_{i_j} are called* inner corners *at O_{i_j}. An element $\mathbf{x} \in \mathbf{S}(G)$ is called* inner *if, for each $j = 1, \dots, k$, at least one of the inner corners at O_{i_j} is part of $\mathbf{x}$. The element $\mathbf{x}$ is called* outer *otherwise.*

Lemma 5.2. *Let $(G, \mathcal{Z})$ be a sparse toroidal grid diagram with some O's marked for destabilization, where $|\mathcal{Z}| = k \geq 2$. Let $\mathbf{p} = [\mathbf{x}, \tilde{\mathbf{y}}]$ be a positive pair such that $\mathbf{x}$ is inner. Then the index $I(\mathbf{p})$ is at least $2 - k$.*

Proof. Let (D, ϵ, ρ) be a positive enhanced domain going between $\mathbf{x}$ and $\tilde{\mathbf{y}}$. Then

$$I(\mathbf{p}) = I(D, \epsilon, \rho) = I(D) - \sum_{j=1}^{k} (\epsilon_j + 2f_j)$$

by Equation (24).

Just as in the proof of Proposition 3.6, without loss of generality we can assume that every row or column contains at least one square where the multiplicity of D is zero; hence, as we move to an adjacent row (or column), the multiplicity of the domain D can only change by 0 or ± 1.

According to Equation (25), the usual index $I(D)$ is given by the sum of the average multiplicities of D at the corners. For each $j = 1, \dots, k$, define n_j to be the sum of the average multiplicities at the corners situated on one of the following four lines: the two vertical lines bordering the column of O_{i_j} and the two horizontal lines bordering the row of O_{i_j}; with the caveat that, if such a corner c (with average multiplicity a around it) appears on one of the four lines for O_{i_j} and also on one of the four lines for O_{i_l}, $l \neq j$, then we let c contribute $a/2$ to n_j and $a/2$ to n_l. For an example, see Figure 10. Note that, since the diagram is sparse, the average multiplicities at inner corners are only counted in one n_l.

We get

$$I(\mathbf{p}) \geq \sum_{j=1}^{k} (n_j - \epsilon_j - 2f_j). \tag{44}$$

We will prove that

$$n_j \geq 2f_j + \epsilon_j/2. \tag{45}$$

Indeed, the relations (28) imply that the average multiplicity at the destabilization point p_j for O_{i_j} (which is part of $\mathbf{y}$) is

$$\frac{a_j + b_j + c_j + d_j}{4} \geq f_j + \frac{2\epsilon_j - 1}{4}.$$

Since $\mathbf{x}$ is inner, there is also one point of $\mathbf{x}$, call it x, in a corner of the square containing O_{i_j}. There are four cases, according to the position of x. We first consider the case when the marking at O_{i_j} is L (i.e., $\epsilon_j = 0$).

1. If x is the lower left corner (which is the same as the destabilization point), we have $a_j + d_j = b_j + c_j \geq 2f_j$ there, so the average multiplicity at x is at least f_j; since the corner counts in both $\mathbf{x}$ and $\mathbf{y}$, we get $n_j \geq 2f_j$, as desired.
2. If x is the lower right corner, since $b_j, d_j \geq f_j$ and the multiplicity of D can change by at most ± 1 as we pass a column, we find that the average multiplicity at x is at least $f_j - 1/4$. Together with the contribution from $p_j \in \mathbf{y}$, this adds up to $2f_j - 1/2$. Suppose both the contributions from p_j and x are exactly $f_j - 1/4$. Then if r is a square other than O_j in the row through O_j, and s is the square directly below it, the local multiplicity at r is one greater than it is at s. This contradicts the positivity assumption combined with the

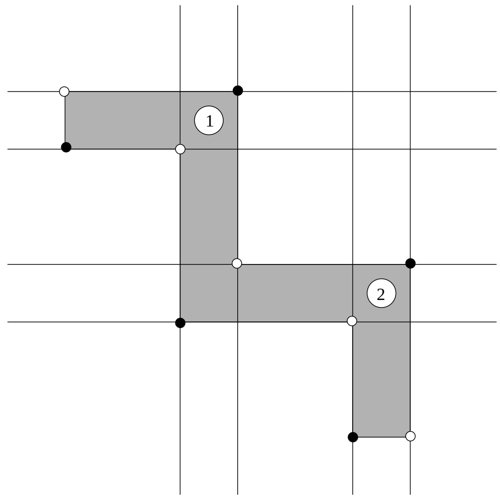

FIGURE 10. **An example of a positive enhanced domain with x inner.** We have $k = 2$ and the two O's marked for destabilization ($O_{i_j}, j = 1, 2$) are shown in the figure with the value of j written inside. We view this as a domain of type LL, meaning that $\epsilon_1 = \epsilon_2 = 0$, and with the real multiplicities at the destabilization points equal to zero, so that $f_1 = f_2 = 1$. The domain has index 0, and the quantities n_1 and n_2 both equal $3 \cdot (1/4) + (3/4) + (1/4 + 3/4)/2 = 2$.

assumption that there is at least one square with multiplicity 0 in the row containing O_j. Hence, the contribution from x and p_j is at least $2f_j$, as desired.

(3) The case when x is the upper left corner is similar to lower right, with the roles of the the row and the column through O_{i_j} swapped.

(4) Finally, if x is the upper right corner, then the average multiplicity there is at least $f_j - 3/4$. Together with the contribution from $p_j \in \mathbf{y}$, we get a contribution of at least $2f_j - 1$. There are two remaining corners on the vertical lines through p_j and x; we call them $c_1 \in \mathbf{x}$ and $c_2 \in \mathbf{y}$, respectively. We claim that the contributions of the average multiplicities of c_1 and c_2 to n_j sum up to at least $1/2$. Indeed, if at least one of these average multiplicities is $\geq 3/4$, their sum is ≥ 1, which might be halved (because the contribution may be split with another n_l) to get at least $1/2$. If both of the average multiplicities are $1/4$ (i.e., both c_1 and c_2 are $90°$ corners), they must lie on the same horizontal line, and therefore their contributions are not shared with any of the other n_l's; so they still add up to $1/2$. A similar argument gives an additional contribution of at least $1/2$ from the two remaining corners on the row through O_{i_j}. Adding it all up, we get $n_j \geq (2f_j - 1) + 1/2 + 1/2 = 2f_j$.

This completes the proof of Equation (45) when D is of type L at O_{i_j}. When D is of type R there (i.e., $\epsilon_j = 1$), the contribution of x to n_j is at least $f_j - \frac{3}{4}$. Studying the four possible positions of x, just as in the L case, gives additional contributions to n_j of at least 1, which proves Equation (45). In fact, the contributions are typically strictly greater than 1; the only situation in which we can have equality in (45) when D is of type R is when x is the upper right corner and the local multiplicities around x and p_j are exactly as in Figure 11.

Putting Equation (45) together with Inequality (44), we obtain

$$I(\mathbf{p}) \geq \sum_{j=1}^{k} (-\epsilon_j/2) \geq -k/2. \tag{46}$$

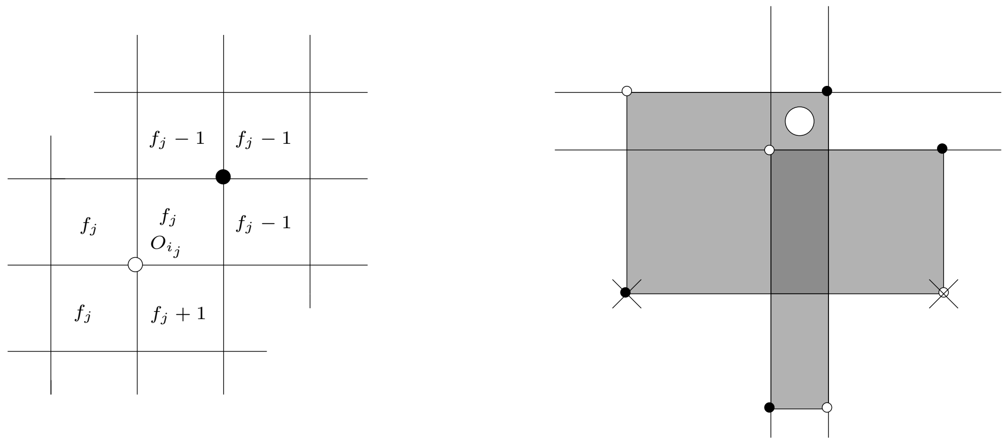

FIGURE 11. **Equality in Equation** (45)**.** On the left, we show the local multiplicities around O_{i_j} in the case $\epsilon_j = 1, n_j = 2f_j + 1/2$. (Note that the real multiplicity at O_{i_j} is then zero.) On the right we picture a domain of this type, with $k = 1$, $f_1 = 1$. There are two corners, marked by $\times$, whose contributions are not counted in n_1. As a consequence, the Inequality (44) is strict.

Our goal was to show that $I(\mathbf{p}) \geq 2 - k$. This follows directly from (46) for $k \geq 4$; it also follows when $k = 3$, by observing that $I(\mathbf{p})$ is an integer.

The only remaining case is $k = 2$, when we want to show $I(\mathbf{p}) \geq 0$, but Inequality (46) only gives $I(\mathbf{p}) \geq -1$. However, if $I(\mathbf{p}) = -1$ we would have equality in all inequalities that were used to arrive at Inequality (46). In particular, both destabilizations are of type R, the corresponding x's are the upper right corners of the respective squares, and the local multiplicities there are as in Figure 11. Observe that as we move down from the row above O_{i_j} to the row containing O_{i_j}, the local multiplicity cannot decrease. The same is true as we move down from the row containing O_{i_j} to the one just below. On the other hand, looking at the column of O_{i_1}, as we go down around the grid from the square just below O_{i_1} (where the multiplicity is $f_1 + 1$) to the one just above O_{i_1} (where the multiplicity is $f_j - 1$), we must encounter at least two horizontal circles where the multiplicity decreases. By our observation above, neither of these circles can be one of the two that bound the row through O_{i_2}. However, one or two of them could be the circles of the two remaining corners on the column through O_{i_1}. These corners only contribute to n_1, not to n_2, and since we had equality when we counted their contribution to be at least $1/2$, it must be the case that each of them is a 90° corner, with a contribution of $1/4$. This means that they must lie on the same horizontal circle. Hence, there must be one other horizontal circle along which local multiplicities of our domain decrease as we cross it from above. On this circle there are some additional corners, with a nontrivial contribution to $I(D)$ unaccounted for; compare the right hand side of Figure 11. (Note however that in that figure, we consider $k = 1$, rather than $k = 2$.) These vertices contribute extra to the vertex multiplicity, which means that $I(\mathbf{p}) > -1$. $\square$

Remark 5.3. It may be possible to improve the inequality (46) to $I(\mathbf{p}) \geq 0$ for every $k > 0$ along the same lines, by doing a more careful analysis of the contributions to $I(D)$.

Lemma 5.4. *Let $(G, \mathcal{Z})$ be a sparse toroidal grid diagram, and $\mathbf{p} = [\mathbf{x}, \tilde{\mathbf{y}}]$ a positive pair such that $\mathbf{x}$ is outer. Then the cohomology of $C\mathcal{F}^*(G, \mathcal{Z}, \mathbf{p})$ is zero.*

Proof. First, observe that, since the differential of $\mathrm{gr}_{\mathcal{F}}\, CP^*(G, \mathcal{Z})$ only involves pre-compositions, $\tilde{\mathbf{y}}$ is the same for all generators of $C\mathcal{F}^*(G, \mathcal{Z}, \mathbf{p})$. Furthermore, since $\mathbf{x}$ is outer, all the other generators $[\mathbf{x}', \tilde{\mathbf{y}}]$ of $C\mathcal{F}^*(G, \mathcal{Z}, \mathbf{p})$ are outer.

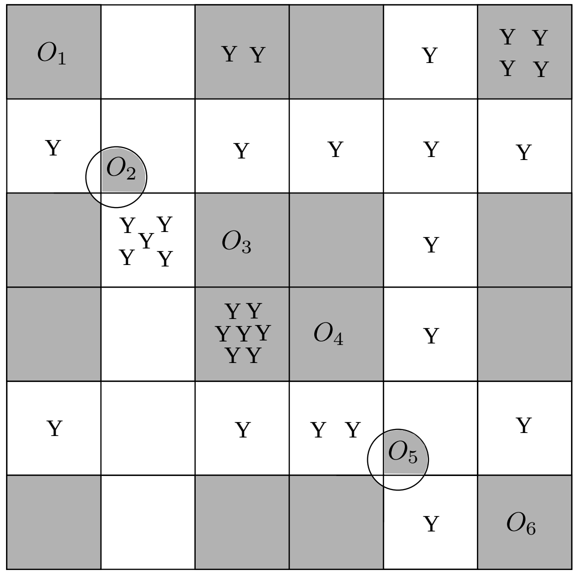

FIGURE 12. **The markings defining the filtrations.** We show here a grid diagram of grid number 6, with two O's marked for destabilization, namely $O_{i_1} = O_2$ and $O_{i_2} = O_5$. We draw small circles surrounding each of the two destabilization points. Each shaded square contains an X and this defines the filtration $\mathcal{F}$. One could also imagine an X marking in the upper right quadrant of each small destabilization disk, to account for the term ρ_j in Equation (43). Given an outer generator $\mathbf{x}$, we need to choose some $j \in \{1, 2\}$ such that no corner O_{i_j} is in $\mathbf{x}$. Suppose we chose $j = 1$. We then define a second filtration $\mathcal{G}$ on the components of the associated graded of $\mathcal{F}$, using the Y markings as shown, plus five (invisible) Y markings in the lower left corner of each small destabilization disk. We first choose the Y markings in the unshaded squares, then mark the shaded squares so that every periodic domain has a total of zero markings, counted with multiplicities.

Let j be such that no corner of O_{i_j} is in $\mathbf{x}$. Consider a new filtration $\mathcal{G}$ on $C\mathcal{F}^*(G, \mathcal{Z}, \mathbf{p})$ given as follows. Let us mark one Y in each square of the grid that lies in a column or row through an O marked for destabilization, but does not lie in the column going though O_{i_j} (where j was chosen above), nor does it lie in the same square as one of the other O_{i_l}'s. Further, we mark $n - 1$ copies of Y in the square directly below the square of O_{i_j}. (Here n is the size of the grid.) Finally, we mark one extra Y in the square directly to the left of each O_{i_l}, $l \neq j$. See Figure 12 for an example. Observe that for every periodic domain equal to the row through some O_{i_l} minus the column through O_{i_l} (for some $l = 1, \ldots, k$, including $l = j$), the signed count of Y's in that domain is zero.

Consider now the squares in G that do not lie in any row or column that goes through an O marked for destabilization. We denote them by $s_{u,v}$, with $u, v \in \{1, \ldots, n - k\}$, where the two indices u and v keep track of the (renumbered) row and column, respectively. Note that all these squares are already marked by an X, used to define the filtration $\mathcal{F}$. We will additionally mark them with several Y's, where the exact number $\alpha_{i,j}$ of Y's in $s_{i,j}$ is to be specified soon.

Given one of the generators $\mathbf{p}' = [\mathbf{x}', \tilde{\mathbf{y}}]$ of $C\mathcal{F}^*(G, \mathcal{Z}, \mathbf{p})$, choose an enhanced domain (D, ϵ, ρ) from $\mathbf{x}'$ to $\mathbf{y}$, and let $Y(D)$ be the number of Y's inside D (counted with multiplicity). Set

$$\mathcal{G}(\mathbf{p}') = -Y(D) - (n-1)\sum_{l=1}^{k}(c_l(D) - f_l(D) - \epsilon_l(D) + 1). \tag{47}$$

Here c_l, f_l, ϵ_l are as in Section 3.2. The second term in the formula above is chosen so that adding to D a column through some O_{i_l} does not change the value of $\mathcal{G}$; this term can be interpreted as marking $n-1$ additional Y's in the lower left quadrant of the small destabilization disk around O_{i_l}.

We require that the quantity $\mathcal{G}$ is well-defined, i.e., it should not depend on D, but only on the pair $\mathbf{p}'$. For this to be true, we need to ensure that the addition of a periodic domain to D does not change $\mathcal{G}$. This can be arranged by a judicious choice of the quantities $\alpha_{u,v}$, for $u, v \in \{1, \dots, n-k\}$. Indeed, the only generators of the space of periodic domains that have not been already accounted for are those of the form: column minus row though some O not marked for destabilization. Note that there is a permutation σ of $\{1, \dots, n-k\}$ such that the unmarked O's are in the squares $s_{u\sigma(u)}$. There are $n-k$ conditions that we need to impose on $\alpha_{u,v}$, namely

$$\sum_{v=1}^{n-k}\alpha_{uv} - \sum_{v=1}^{n-k}\alpha_{v\sigma(u)} = t_u, \tag{48}$$

for $u = 1, \dots, n-k$. Here t_u are determined by the number of Y's that we already marked in the respective row and column (as specified above, in squares not marked by X), with an extra contribution in the case of the row just below some O_{i_l} and the column just to the left of O_{i_l}, to account for the term $c_l(D) - f_l(D) - \epsilon_l(D) + 1$ from Equation (47).

Note that $\sum_{u=1}^{n-k} t_u = 0$. We claim that there exists a solution (in rational numbers) to the linear system described in Equation (48). Indeed, the system is described by a $(n-k)$-by-$(n-k)^2$ matrix A, each of whose columns contains one 1 entry, one -1 entry, and the rest just zeros. If a vector $(\beta_u)_{u=1,\dots,n-k}$ is in the kernel of the transpose A^t, it must have $\beta_u - \beta_v = 0$ for all u, v. In other words, $\mathrm{Im}(A)^\perp = \mathrm{Ker}(A^t)$ is the span of $(1, \dots, 1)$, so $(t_1, \dots, t_{n-k})$ must be in the image of A.

By multiplying all the values in a rational solution of (48) by a large integer (and also multiplying the number of Y's initially placed in the rows and columns of the destabilized O's by the same integer), we can obtain a solution of (48) in integers. By adding a sufficiently large constant to the α_{uv} (but not to the number of Y's initially placed), we can then obtain a solution in nonnegative integers, which we take to be our definition of α_{uv}.

We have now arranged so that $\mathcal{G}$ is an invariant of $\mathbf{p}'$. Moreover, pre-composing with a rectangle can only decrease $\mathcal{G}$, and it keeps $\mathcal{G}$ the same only when the rectangle (which a priori has to be supported in one of the rows and columns through some O_{i_l}) is actually supported in the column through O_{i_j}, and does not contain the square right below O_{i_l}.

It follows that $\mathcal{G}$ is indeed a filtration on $C\mathcal{F}^*(G, \mathcal{Z}, \mathbf{p})$. We denote the connected components of the associated graded complex by $C\mathcal{G}^*(G, \mathcal{Z}, \mathbf{p}')$; it suffices to show that these have zero cohomology. Without loss of generality, we will focus on $C\mathcal{G}^*(G, \mathcal{Z}, \mathbf{p})$.

The complex $C\mathcal{G}^*(G, \mathcal{Z}, \mathbf{p})$ can only contain pairs $[\mathbf{x}', \tilde{\mathbf{y}}]$ such that $\mathbf{x}'$ differs from $\mathbf{x}$ by either pre- or post-composition with a rectangle supported in the column through O_{i_j}. The condition that this rectangle does not contain the square right below O_{i_l} is automatic, because $\mathbf{x}$ and $\mathbf{x}'$ are outer.

We find that there can be at most two elements in $C\mathcal{G}^*(G, \mathcal{Z}, \mathbf{p})$, namely $\mathbf{p} = [\mathbf{x}, \tilde{\mathbf{y}}]$ and $\mathbf{p}' = [\mathbf{x}', \tilde{\mathbf{y}}]$, where $\mathbf{x}'$ is obtained from $\mathbf{x}$ by switching the horizontal coordinates of the components of $\mathbf{x}$ in the two vertical circles bordering the column of O_{i_j}. Provided that $\mathbf{p}'$ is positive, the pairs $\mathbf{p}$ and $\mathbf{p}'$ are related by a differential, so the cohomology of $C\mathcal{G}^*(G, \mathcal{Z}, \mathbf{p})$ would indeed be zero.

Therefore, the last thing to be checked is that $\mathbf{p}'$ is positive. We know that $\mathbf{p}$ is positive, so we can choose a positive enhanced domain D representing $\mathbf{p}$. Recall that the destabilization point near

O_{i_j} is denoted p_j and is part of $\mathbf{y}$. Draw a vertical segment S going down the vertical circle from p_j to a point of $\mathbf{x}$. There are three cases:

(1) There is no point of $\mathbf{x}'$ on the segment S. Then there exists a rectangle going from $\mathbf{x}'$ to $\mathbf{x}$, and $\mathbf{p}'$ appears in $d\mathbf{p}$ by pre-composition. Adding the rectangle to D preserves positivity.

(2) There is a point of $\mathbf{x}'$ on S, and the multiplicity of D just to the right of S is nonnegative. Then there is a rectangle, just to the right of S, going from $\mathbf{x}$ to $\mathbf{x}'$. We get a positive representative for $\mathbf{p}'$ by subtracting this rectangle from D.

(3) There is a point of $\mathbf{x}'$ on S, and the multiplicity of D is zero somewhere just to the right of S. Note that as we cross the segment S from left to right the drop in multiplicity is constant; since D is positive, this drop must be nonnegative. In particular, $c_j \geq d_j$. Relation (26) implies $a_j \geq b_j + 1$. Looking at the inequalities in (28), we see that we can use two of them (the ones involving b_j and d_j) to improve the other two:

$$a_j \geq b_j + 1 \geq f_j + 1, \qquad c_j \geq d_j \geq f_j + \epsilon_j. \tag{49}$$

Let us add to D the periodic domain given by the column through O_{i_j}. This increases b_j, d_j, and f_j by 1 while keeping a_j and c_j constant. Nevertheless, Inequality (49) shows that the inequalities (28) are still satisfied for the new domain $\tilde{D}$. Thus $\tilde{D}$ is positive, and its multiplicity just to the right of S is everywhere nonnegative. We can then subtract a rectangle from $\tilde{D}$ to obtain a positive representative for $\mathbf{p}'$ as in case (2).

The three cases are pictured in Figure 13. □

Proof of Theorem 4.3. The case when $k = 0$ is trivial, and the case $k = 1$ follows from Proposition 3.6. For $k \geq 2$, Lemma 5.2 says that for any pair $[\mathbf{x}, \tilde{\mathbf{y}}]$ of index $< 2 - k$, the generator $\mathbf{x}$ is outer. Lemma 5.4 then shows that the homology of $\mathrm{gr}_{\mathcal{F}}\, CP^*(G, \mathcal{Z})$ is zero in the given range, which implies the same for $HP^*(G, \mathcal{Z})$. □

References

[1] J. A. Baldwin and W. D. Gillam, *Computations of Heegaard-Floer knot homology*, preprint, `arXiv:math.GT/0610167`.

[2] A. Beliakova, *A simplification of combinatorial link Floer homology*, J. Knot Theory Ramifications, **19**(2010), no. 2, 125–144, `arXiv:0705.0669`.

[3] S. K. Donaldson, *An application of gauge theory to four-dimensional topology*, J. Differential Geom., **18**(1983), no. 2, 279–315.

[4] S. K. Donaldson, *Polynomial invariants for smooth four-manifolds*, Topology, **29**(1990), no. 3, 257–315.

[5] J.-M. Droz, *Effective computation of knot Floer homology*, Acta Math. Vietnam., **33**(2008), no. 3, 471–491, `arXiv:0803.2379`.

[6] P. Kronheimer and T. Mrowka, *Monopoles and three-manifolds*, volume 10 of *New Mathematical Monographs*, Cambridge University Press, Cambridge, 2007.

[7] R. Lipshitz, *A cylindrical reformulation of Heegaard Floer homology*, Geom. Topol., **10**(2006), 955–1097, `arXiv:math.SG/0502404`.

[8] R. Lipshitz, C. Manolescu, and J. Wang, *Combinatorial cobordism maps in hat Heegaard Floer theory*, Duke Math. J., **145**(2008), no. 2, 207–247, `arXiv:math/0611927`.

[9] R. Lipshitz, P. S. Ozsváth, and D. P. Thurston, *Bordered Floer homology and the branched double cover I*, preprint (2010), `arXiv:1011.0499`.

[10] R. Lipshitz, P. S. Ozsváth, and D. P. Thurston, *Bordered Floer homology and the branched double cover II: the spectral sequences agree*, in preparation.

[11] R. Lipshitz, P. S. Ozsváth, and D. P. Thurston, *Computing $\widehat{HF}$ by factoring mapping classes*, preprint (2010), `arXiv:1010.2550`.

[12] C. Manolescu and P. S. Ozsváth, *Heegaard Floer homology and integer surgeries on links*, preprint (2010), `arXiv:1011.1317`.

[13] C. Manolescu, P. S. Ozsváth, and S. Sarkar, *A combinatorial description of knot Floer homology*, Ann. of Math. (2), **169**(2009), no. 2, 633–660, `arXiv:math.GT/0607691`.

[14] C. Manolescu, P. S. Ozsváth, Z. Szabó, and D. P. Thurston, *On combinatorial link Floer homology*, Geom. Topol., **11**(2007), 2339–2412, `arXiv:math.GT/0610559`.

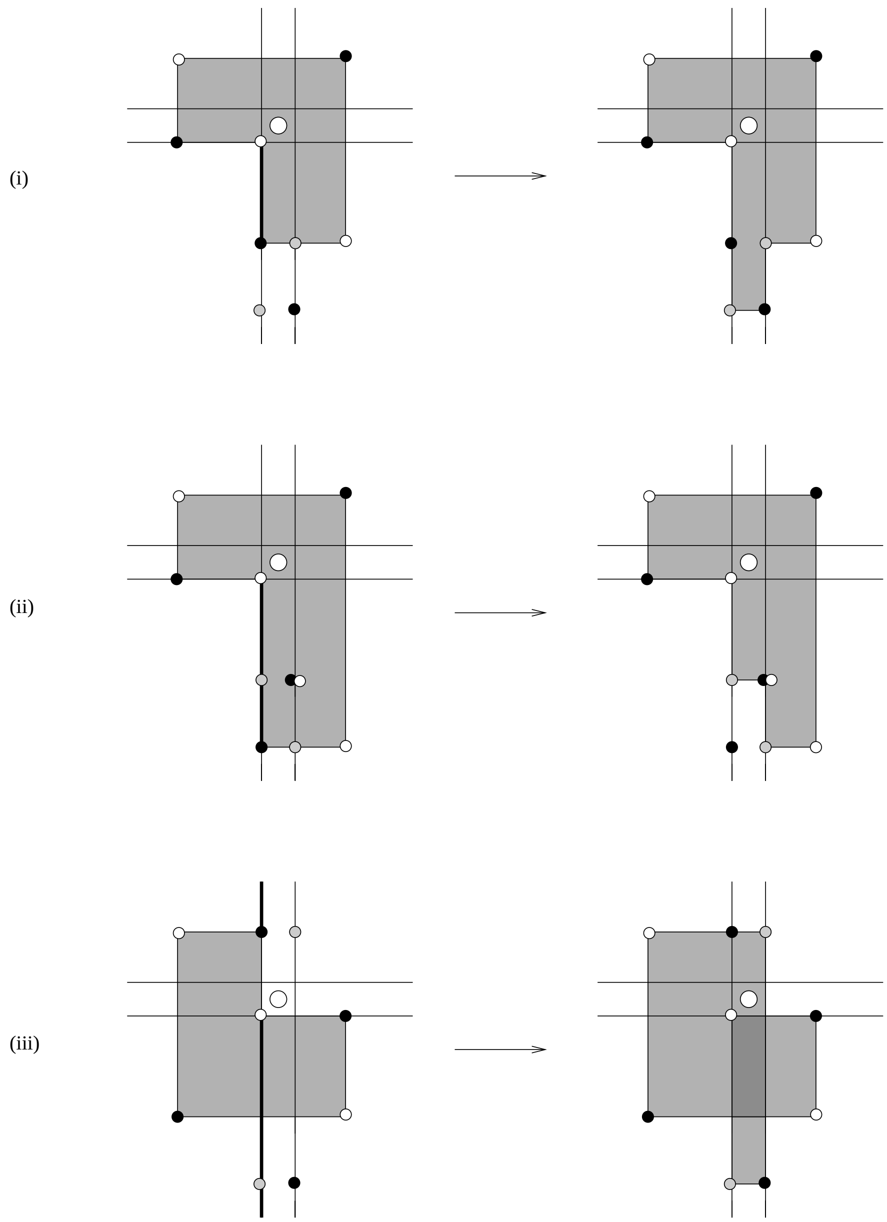

FIGURE 13. **The three cases in Lemma 5.4.** On the left of each picture we show a positive L domain representing $\mathbf{p} = [\mathbf{x}, \tilde{\mathbf{y}}]$. These domains have index 0, 2 and 2, respectively (assuming that all the real multiplicities are zero). On the right of each picture we show the corresponding positive domain representing $\mathbf{p}' = [\mathbf{x}', \tilde{\mathbf{y}}]$. These domains have all index 1. The components of $\mathbf{x}$ are the black dots, the components of $\mathbf{x}'$ the gray dots, and those of $\mathbf{y}$ the white dots. The segment S is drawn thicker.

[15] Y. Ni, *Heegaard Floer homology and fibred 3-manifolds*, Amer. J. Math., **131**(2009), no. 4, 1047–1063, `arXiv:0706.2032`.

[16] P. Ozsváth and Z. Szabó, *A cube of resolutions for knot Floer homology*, J. Topol., **2**(2009), no. 4, 865–910, `arXiv:0705.3852`.

[17] P. S. Ozsváth, A. Stipsicz, and Z. Szabó, *A combinatorial description of the $U^2 = 0$ version of Heegaard Floer homology*, preprint (2008), `arXiv:0811.3395`.

[18] P. S. Ozsváth and Z. Szabó, *Knot Floer homology and rational surgeries*, preprint (2005), `arXiv:math.GT/0504404`.
[19] P. S. Ozsváth and Z. Szabó, *Holomorphic disks and genus bounds*, Geom. Topol., **8**(2004), 311–334, `arXiv:math.GT/0311496`.
[20] P. S. Ozsváth and Z. Szabó, *Holomorphic disks and knot invariants*, Adv. Math., **186**(2004), no. 1, 58–116, `arXiv:math.GT/0209056`.
[21] P. S. Ozsváth and Z. Szabó, *Holomorphic disks and three-manifold invariants: properties and applications*, Ann. of Math. (2), **159**(2004), no. 3, 1159–1245, `arXiv:math.SG/0105202`.
[22] P. S. Ozsváth and Z. Szabó, *Holomorphic disks and topological invariants for closed three-manifolds*, Ann. of Math. (2), **159**(2004), no. 3, 1027–1158, `arXiv:math.SG/0101206`.
[23] P. S. Ozsváth and Z. Szabó, *On the Heegaard Floer homology of branched double-covers*, Adv. Math., **194**(2005), no. 1, 1–33, `arXiv:math.GT/0309170`.
[24] P. S. Ozsváth and Z. Szabó, *Holomorphic triangles and invariants for smooth four-manifolds*, Adv. Math., **202**(2006), no. 2, 326–400, `arXiv:math.SG/0110169`.
[25] P. S. Ozsváth and Z. Szabó, *Holomorphic disks, link invariants and the multi-variable Alexander polynomial*, Algebr. Geom. Topol., **8**(2008), no. 2, 615–692, `arXiv:math/0512286`.
[26] P. S. Ozsváth and Z. Szabó, *Knot Floer homology and integer surgeries*, Algebr. Geom. Topol., **8**(2008), no. 1, 101–153, `arXiv:math/0410300`.
[27] J. A. Rasmussen, *Floer homology and knot complements*, Ph.D. thesis, Harvard University, 2003, `arXiv:math.GT/0306378`.
[28] S. Sarkar and J. Wang, *An algorithm for computing some Heegaard Floer homologies*, Ann. of Math. (2), **171**(2010), no. 2, 1213–1236, `arXiv:math/0607777`.
[29] N. Seiberg and E. Witten, *Electric-magnetic duality, monopole condensation, and confinement in $N = 2$ supersymmetric Yang-Mills theory*, Nuclear Phys. B, **426**(1994), no. 1, 19–52, `arXiv:hep-th/9407087`.
[30] N. Seiberg and E. Witten, *Monopoles, duality and chiral symmetry breaking in $N = 2$ supersymmetric QCD*, Nuclear Phys. B, **431**(1994), no. 3, 484–550, `arXiv:hep-th/9408074`.
[31] E. Witten, *Monopoles and four-manifolds*, Math. Res. Lett., **1**(1994), 769–796, `arXiv:hep-th/9411102`.

Department of Mathematics, UCLA, 520 Portola Plaza, Los Angeles, CA 90095
E-mail address: `cm@math.ucla.edu`

Department of Mathematics, Massachusetts Institute of Technology, Cambridge, MA 02139
E-mail address: `petero@math.mit.edu`

Department of Mathematics, Barnard College, Columbia University, New York, NY 10027
E-mail address: `dthurston@barnard.edu`